Targeting dendritic cells with a PD-L1 based bispecific antibody rejuvenates specific anti-tumor T cells

Longchao Liu
UT southwestern medical center https://orcid.org/0000-0003-3394-5919
Jiahui Chen
UT southwestern medical center
Joonbeom Bae
UT southwestern medical center
Zhida Liu
The University of Texas Southwestern Medical Center https://orcid.org/0000-0002-3980-8440
Eric Hsu
UT southwestern medical center https://orcid.org/0000-0002-6743-2399
Chuanhui Han
UT southwestern medical center
Changzheng Lu
UT southwestern medical center
Jian Qiao
UT southwestern medical center
yang-xin fu (yang-xin.fu@utsouthwestern.edu)
UT southwestern medical center https://orcid.org/0000-0002-4809-825X

Article

Keywords: Bispecific antibody, immunotherapy, PD-L1, dendritic cell, co-stimulatory signaling, antigen-25 specific T cell, anti-tumor immunity, checkpoint blockade

Posted Date: July 23rd, 2020

DOI: https://doi.org/10.21203/rs.3.rs-39214/v1

Version of Record: A version of this preprint was published at Nature Biomedical Engineering on November 1st, 2021. See the published version at https://doi.org/10.1038/s41551-021-00800-2.

Targeting dendritic cells with a PD-L1 based bispecific antibody rejuvenates specific anti-tumor T cells

Longchao Liu[1], Jiahui Chen[2], Joonbeom Bae[1], Zhida Liu[1], Eric Hsu[1], Chuanhui Han[1], Changzheng Lu[1], Jian Qiao, and Yang-Xin Fu[1,*]

[1]Department of Pathology, UT Southwestern Medical Center, Dallas, TX 75390, USA

[2]Harold C. Simmons Comprehensive Cancer Center, University of Texas Southwestern Medical Center, Dallas, TX 75390, USA

*Correspondence: Yang-Xin.Fu@UTSouthwestern.edu (Y.-X. F.)

Abstract

Bispecific T-cell engagers (BiTEs) that preferentially target tumor-associated antigens (TAA) to reengage CD3 signaling have been approved to treat acute B-cell lymphoblastic leukemia. However, their applications in solid tumors have been hampered due to short half-life, weak anti-tumor activity, and severe toxicity at therapeutic doses. To explore new targets, we designed a bispecific antibody (BsAb) which simultaneously targets CD3 and immune checkpoint PD-L1. Compared with conventional TAA based targeting, PDL1xCD3 generates far superior anti-tumor immune responses *in vivo*. Mechanistically, blockade of PD-L1 on dendritic cells instead of tumor cells can potently rejuvenate preexisting tumor reactive CD8 T cells in a B7-1/2 dependent manner for a durable anti-tumor responses. This study argues that targeting DC-T cell instead of current tumor-T cell can achieve much better T cell rejuvenation in BsAb therapy.

Keywords

Bispecific antibody, immunotherapy, PD-L1, dendritic cell, co-stimulatory signaling, antigen-specific T cell, anti-tumor immunity, checkpoint blockade

Introduction

Therapeutic strategies aiming to redirect T cells in the tumor have been increasingly studied in multiple cancer types over the past decades[1-4]. Bispecific T cell engager (BiTE), which simultaneously binds tumor-associated antigen (TAA) and CD3ε is one of the most potent technology that can redirect T cells in the tumor tissue to cancer cells regardless of their intrinsic TCRs. Despite the success application of blinatumomab, a U.S. Food and Drug Administration (FDA) approved BiTE for patient with B-cell precursor acute lymphoblastic leukemia (BCP ALL) in first or second complete remission with minimal residual disease (MRD) [5,6]. The application of BiTEs on solid tumors has been hampered, presumably due to their short *in vivo* half-life and severe side effects[7-9]. The *in vivo* efficacy of the fusion protein mainly depends on the specificity of TAAs, which usually have an expression on noncancerous tissue as well. Extensive efforts have been made to discover appropriate targets on tumor cells, such as the EGFRxCD3, EpCAMxCD3 and Her2xCD3[10-12]. However, it is clear that the CD3 signal still get cross-linked with such TAAs in peripheral noncancerous tissue, causing "on-target off-tumor" distractions and severe toxicity in the form of cytokine storm and tissue damage[13]. In addition, it is still unclear whether such BiTEs can generate tumor specific memory responses. Generally, current BiTEs are evaluated in xenograft mouse models, where human tumors and PBMCs are presented in the immune-deficient host. However, such xenograft models fail to recapitulate "on-target off-tumor" distractions and severe toxicity because human antigens are not presented on the non-tumor mouse cells. It is also difficult to evaluate memory responses due to the nature of Graft-Versus-Host Disease effects by PBMCs. Therefore, the efficacy of BiTEs can be overestimated while toxicity is far underestimated. Severe side effects have been observed in clinical trials of BiTEs despite the promising efficacy evaluated in xenograft mouse models. Optimized strategies or targets should be developed to overcome this primary barrier[14,15].

The TCR signaling threshold can determine the fate of T cell activation [16]. Insufficient TCR stimulation and lack of co-stimulatory engagement with professional antigen presenting cells (APCs) can lead to T cell exhaustion[17,18]. In addition, TCR stimulation alone can cause activation-induced cell death (AICD) [19]. During natural T cell priming, APCs especially DCs can provide three signals for proper T cell activation and survival. The TCR engagement of peptide-MHC (signal 1), co-stimulation between B7 and CD28 (signal 2), and inflammatory cytokines IL2, IL12

or type I IFN (signal 3) [20]. To mimic this natural interaction, chimeric antigen receptor T cells (CAR-T) are designed to provide both signal 1 (via a portion of the CD3ζ cytodomain) and signal 2 (via a portion of the CD28 cytodomain)[21,22]. However, treatment with BiTEs can only trigger TCR engagement and a lack of co-stimulatory signaling leads to T cell apoptosis[23]. Approaches have been implemented to address this issue by providing anti-CD28 simultaneously with BiTE, but it remains unknown whether anti-CD3 and anti-CD28 signaling can efficiently rescue tumor specific T cells[24,25]. Moreover, anti-CD28 signaling can activate a broader range of T cells, leading to acute cytokine storm[26]. Thus, treatments that can provide all three signals for T cell reactivation in the tumor tissue becomes an important paradigm for bispecific antibody design[27].

Since BiTEs reengage CD3 signaling on T cells, any T cell can be activated in spite of their functional properties. CD4 T cells, CD8 T cells, Tregs and NKT cells are highly enriched in the tumor microenvironment, which contributes to the heterogeneity of potentially activated T cells[28]. Thus, it is difficult to determine whether tumor specific or non-specific T cell populations play a dominant role in response to BiTE treatment *in vivo*[29]. Among all T cell populations, antigen specific T cells play an indispensable role of establishing proper anti-tumor immunity, but the percentage of antigen specific T cells are limited in the tumor tissue [30]. Even though BiTE treatment can target tumor cells to activate T cells, the TCR reengagement is non-specific. Bystander T cells rather than antigen specific T cells could be preferentially activated due to their high abundance and less exhausted phenotype. Furthermore, studies have shown that CD8 T cells within the tumor consist of distinct populations of terminally differentiated and stem-like cells, the latter of which have an effector-molecule secretion potential and reside in APC niches[31]. Thus, targeting APCs to engage T cells should be considered as a potential strategy to rejuvenate specific anti-tumor T cell immunity.

Meanwhile, many types of immune cells (such as myeloid-derived suppressor cells, macrophages and regulatory T cells) and tumor cells create an immune-resistant tumor microenvironment by providing co-inhibitory signals such as programmed death-ligand 1 (PD-L1). PD-L1 can inhibit the function of CD8 T cells at either the cytotoxic stage or re-activation stage[32-34]. Effector molecules, like IFNγ, that are released after T cell engagement also upregulate the expression of PD-L1, which further promotes adaptive resistance to BiTE treatment [35,36]. Thus

the therapeutic effect of BiTE treatment can be improved in combination with checkpoint blockade [37].

To overcome the limitations of current tumor cell targeting BiTE therapy, we designed a novel bispecific antibody that targets immune checkpoint PD-L1 to redirect T cells to APCs. We unexpectedly observed that PDL1xCD3 generates much better anti-tumor effect than conventional TAA targeting bispecific antibody (EGFRxCD3) *in vivo*. We also reveal a new target on APCs to rejuvenate T cells by reducing inhibition and enhancing B7/CD28 co-stimulation. Therefore, this study opens new targets to overcome major hurdles encountered in the current dogma of bispecific T-cell engager therapies.

Results

PDL1xCD3 targets PD-L1 to activate T cells *in vitro*

In order to compare the anti-tumor efficacy of TAA-targeting T cell engagers with PD-L1-targeting T cell engagers, we generated two different types of bispecific antibodies. One targets the human epidermal growth factor receptor (EGFR) and murine CD3ε, while the other targets PD-L1 and murine CD3ε. Both antibodies consist of two single-chain variable fragments (ScFv, anti-EGFR from Cetuximab, anti-PD-L1 from Atezolizumab, anti-CD3 from clone 17A2) and an Fc domain of human IgG1 that prolongs protein half-life *in vivo*. The CH3 domains of the antibodies were engineered with 'Knobs-into-holes' mutants to form heterodimers and the CH2 domains were engineered with 'LALA-PG' mutants to reduce Fc γ receptor (FcγR) binding (Figure 1A and S1A) [38,39]. We first confirmed the purity and molecular weight of the bispecific antibodies by gel electrophoresis under reducing and non-reducing conditions (Figure S1B). Then, to compare the binding affinity and therapeutic effects of each bispecific antibody, we derived a new target cell line from the murine colorectal cancer cell line MC38[40]. This cell line, termed MC38E5, expresses a chimeric EGFR with six amino acids mutated from full-length mouse EGFR. This mutant motif can be recognized by the anti-EGFR antibody. The PD-L1 targeting fusion protein (PDL1xCD3) can specifically bind to PD-L1$^+$ tumor cells, whereas the EGFR targeting fusion protein (ErbxCD3) preferentially binds to EGFR$^+$ tumor cells (Figure 1B-1C). Furthermore, both antibodies have similar affinity to CD3ε on naïve CD8 T cells (Figure 1D).

The Fc domain plays controversial roles on bispecific antibody function. On one hand it prolong *in vivo* half-life; on the other hand it also non-specifically cross-links CD3 signaling. We have observed that antibody-dependent cellular cytotoxicity (ADCC) effect also depletes T cells instead of expanding them (Figure S1C-S1D). Thus, we re-engineered the Fc domain so that FcRn binding affinity is reserved but FcγR binding affinity is reduced. Antibodies with a WT CH2 domain can bind to an FcγR$^+$ murine macrophage cell line. In contrast, antibodies with this re-engineered mutant CH2 domain exhibit a reduced binding affinity which is similar to using anti-CD16/CD32 to block FcγR binding (Figure 1E).

We next tested whether T cells can be activated by bispecific antibodies to kill tumor cells. When antibodies were applied to the co-culture of tumor cells and CD8 T cells, naïve T cells rapidly upregulate the expression of CD25 and CD69 on cell surface with increased secretion of

IFNγ in the supernatant in a dose dependent manner (Figure 1F and 1G). Meanwhile tumor cells were also efficiently killed, indicating a fully functional activation of the T cells (Figure 1H). Even though ErbxCD3 and PDL1xCD3 have similar EC_{50} in T cell activation markers and tumor cell killing, the IFNγ level in PDL1xCD3 group was much higher than that of ErbxCD3 group (Figure 1I). Since T cells express PD-1 upon activation and IFNγ also upregulate PD-L1 on tumor cell, the PD-1/PD-L1 signal may inhibit T cells from secreting IFNγ in ErbxCD3 group[41]. However, in PDL1xCD3 group, the anti-PD-L1 arm of PDL1xCD3 may block this signaling on close proximity to avoid such inhibition. Thus, anti-PD-L1 not only provides a target but also acts as a checkpoint blockade for T cell activation. Furthermore, when PD-L1 was knocked out from tumor cells, PDL1xCD3 completely lost the ability to activate T cells (Figure 1J and 1K). These results demonstrate that PDL1xCD3 can activate T cells to kill tumor cells in a PD-L1 dependent manner *in vitro*.

PDL1xCD3 generates superior anti-tumor effects than TAA-targeting BiTE *in vivo*.

Since PDL1xCD3 generates potent anti-tumor effects *in vitro*, we next investigated whether it can also induce anti-tumor immune responses in syngeneic mouse models. When PDL1xCD3 was administrated intraperitoneally to MC38 bearing mice, tumor was completely eradicated after second infusion. Even though non-specific engagement of CD3 signaling by anti-CD3 displayed similar anti-tumor effect with PDL1xCD3 at early stage, tumor finally relapse after second infusion. Neither anti-PD-L1 single treatment nor anti-PD-L1 + anti-CD3 combination treatment generated anti-tumor effects similar to PDL1xCD3, indicating that the anti-tumor effect of PDL1xCD3 is not due to the synergistic effect of combination treatment (Figure 2A). Moreover, PDL1xCD3 treatment not only improved the overall survival rate but also reduced side effects compared to systemic anti-CD3 treatment (Figure 2B). Mice treated with anti-CD3 lose about 15% of their initial body weight and generate a very strong cytokine storm 24 hours after the first treatment. On the other hand, PD-L1-targeting CD3 engagement by PDL1xCD3 did not cause severe body weight loss nor as high levels of IFNγ, TNFα and IL-6 in the serum as non-targeting anti-CD3 (Figure S2B and S2C). Thus, mice tolerate and respond to PDL1xCD3 treatment very well *in vivo*. Memory T cell responses play a critical role in establishing protective immunity against cancer, but previous studies have shown that BiTE treatment cannot generate memory immune response *in vivo* [42]. We re-challenged PDL1xCD3 cured mice with a 10 fold higher

inoculation of tumor cells on day 50 after treatment. No tumor grew out, indicating that PDL1xCD3 treatment successfully installed memory immune responses after eradicating tumors (Figure 2C). More importantly, PDL1xCD3 treatment also induced OTI-specific IFNγ producing cells in the spleen of MC38OVA bearing mice, further confirmed the efficient generation of antigen specific T cell response (Figure 2D and S1A). Thus, in contrast to convention BiTE, we hypothesized that PDL1xCD3 might provide a distinct signal to T cells, which triggers a specific immune response against tumor without causing severe side effect.

In order to test this hypothesis, we first explored whether PDL1xCD3 could generate superior anti-tumor effect than conventional TAAxCD3. We treated MC38E5 bearing mice with either ErbxCD3 or PDL1xCD3. Even though PDL1xCD3 has similar tumor-killing ability to ErbxCD3 *in vitro*, it displays a much stronger anti-tumor effect *in vivo* (Figure 2E). Consistent results were also observed in cervical cancer model TC-1 expressing chimeric EGFR (TC1E5) (Figure 2G), the breast cancer model TUBO expressing chimeric EGFR (TuBoE5) (Figure S2E) and the melanoma model B16 expressing chimeric EGFR (B16E5) (Figure S2F). In addition, tumor-free mice from PDL1xCD3 treated groups also obtained memory immunity to reject re-challenged tumor cells (Figure 2F and 2H). To exclude the dose effect which may cause ErbxCD3 to be ineffective, we treated mice with ErbxCD3 intratumorally. Even though i.t. injection of ErbxCD3 had an improved anti-tumor effect compared to i.p. injection, the overall anti-tumor effect is still weaker than PDL1xCD3 and no ErbxCD3 treated mice become tumor-free after treatment (Figure S2D). Therefore, dose effects did not contribute to the resistance of ErbxCD3 *in vivo*. Taken together, using syngeneic mouse models of multiple cancer types, we demonstrated PDL1xCD3 generate superior anti-tumor effect than ErbxCD3. These data also raises the possibility that PDL1xCD3 creates a unique microenvironment by engaging different signal pathways or inducing different cell-cell interactions.

Pre-existing CD8 T cells are required for PDL1xCD3 treatment.

Next, we investigated the mechanisms underlying the therapeutic effects of PDL1xCD3. PDL1xCD3 has no effect on MC38 bearing *Rag1*$^{-/-}$ mice, which confirms that adaptive immunity is essential for the therapeutic effect of PDL1xCD3 (Figure 3A). Moreover, CD8 T cells but not CD4 T cells contribute to this effect (Figure 3B). To further determine whether PDL1xCD3 treatment depends on pre-existing T cells in the tumor microenvironment (TME) or recruitment of

T cells from peripheral tissue, we used FTY720, a S1P receptor agonist, to block T cell trafficking to tumor tissue during PDL1xCD3 treatment. As shown in Figure 3C, additional FTY720 blocking did not affect the therapeutic effect of PDL1xCD3, indicating the critical role of pre-existing CD8 T cells in the TME for this treatment. To further clarify whether PDL1xCD3 is targeting tumor tissue to induce the anti-tumor effect, we intratumorally treated mice with the fusion protein. As expect, local treatment was also sufficient to achieve similar anti-tumor effect as systemic treatment (Figure S3A). We also tested the *in vivo* distribution of the fusion protein at different time point post treatment. The antibody was preferentially enriched in the tumor tissue starting at 24 hours post injection and detectable levels were sustained up to day 5 (Figure S3B). Hence, PDL1xCD3 can target tumor tissue to rejuvenate CD8 T cell immunity. Besides CD8 T cells, many other types of immune cell are enriched in the TME in response to treatment. Even though they are not the primary effector cells in tumor killing, they may still play important roles by interacting with CD8 T cells. To identify key components that contribute to the anti-tumor effects during treatment, we applied a series of depleting experiments. NK cell depletion by anti-NK1.1 or macrophage depletion by anti-CSF1R did not affect the therapeutic effect of PDL1xCD3 (Figure 3D). FcγR on host cell also did not play a role during treatment indicating a lack of dependence on ADCC and ADCP (Figure 3E). Since the uniqueness of PDL1xCD3 to ErbxCD3 mainly exists through the targets by which CD3 signaling engages (PD-L1 vs EGFR), we proposed that PD-L1$^+$ cells in the tumor microenvironment may contribute to the CD8 dependent anti-tumor immunity.

PD-L1 on dendritic cells is essential for the anti-tumor effect of PDL1xCD3

PD-L1 is widely expressed by a variety of cell types in multiple tissues including lymphocytes, myeloid cells and tumor cells. To elucidate the role of PD-L1 on different cells in contributing to the PDL1xCD3 treatment, we performed multiple knockout (KO) studies. We first tested the therapeutic effect of PDL1xCD3 on PD-L1 KO tumors. Surprisingly, PDL1xCD3 still generated an effective anti-tumor effect on mice bearing PD-L1 KO MC38 or B16 tumors (Figure 4A and S4C). However, its therapeutic effect was completely abolished on PD-L1 deficient mice bearing WT MC38, indicating that PD-L1 from host cells but not tumor cells play a critical role in the anti-tumor effect of PDL1xCD3 (Figure 4B). To confirm that PD-L1 from tumor cells is not required for the anti-tumor efficacy, we performed a two tumor model experiment. WT and PD-L1 KO MC38 were inoculated on the left and right flank of the mice respectively. PDL1xCD3 treatment

generated equal anti-tumor effect on both tumors irrespective of PD-L1 expression, which further demonstrated the importance of PD-L1 on host cells (Figure S4A and S4B). Since myeloid cells are the dominant host cells that are PD-L1$^+$ in the tumor microenvironment, we next used conditional KO mice to study which PD-L1 cell expressing cells are essential in mediating the anti-tumor effects of PDL1xCD3. Our results showed that, PD-L1 on dendritic cells but not macrophages is required for PDL1xCD3 treatment (Figure 4C and 4D). We have also detected the expression level of PD-L1 on different cells in the tumor. DCs, especially CD103$^+$ DCs expressed the highest level of PD-L1 *in vivo* which may contribute to DC targeting of PDL1xCD3 (Figure S4D). To determine if those DCs are essential, we administered PDL1xCD3 treatment to *Batf3*$^{-/-}$ mice which lack of CD103$^+$ cDC1. Strikingly, the fusion protein completely loses anti-tumor efficacy in those mice despite how few cells are CD103$^+$ in both tumor and draining LN. These results indicate that our treatment may improve CD8 T cell function through a unique subset of DCs (Figure 4E). Taken together, PD-L1 on CD103$^+$ cDC1 plays a critical role in facilitating the anti-tumor effect of PDL1xCD3 treatment.

PDL1xCD3 reshapes a distinct immunophenotypic signature in tumor-bearing mice

Since PDL1xCD3 targets PD-L1 on DCs to facilitate a superior immune response to ErbxCD3, we want to further investigate how the TME is reshaped to promote CD8 T cell responses. Lymphocytes and myeloid cell populations in the spleen and tumor were detected by flow cytometry at 48 hours post treatment. The percentage of CD4 T cells, CD8 T cells and NKT cells in the tumor dramatically increased in PDL1xCD3 but not ErbxCD3 treated group (Figure 5A, S5A and S5B). In contrast, the percentage of NK cell and B cell remains unchanged (Figure S5C and S5D). We further analyzed the immunophenotype of CD8 T cells in the tumor, as they play an essential role during treatment. PDL1xCD3 treatment increased not only CD69 but also Ki-67 expression in CD8 T cells, indicating that CD8 T cells were activated and expanded after treatment (Figure 5B and S5E). The percentage of PD-1 and TIM-3 double positive terminally exhausted CD8 T cells was significantly reduced after treatment, which demonstrates the reversion of immune tolerance in the TME (Figure 5C). Meanwhile, the percentage of TCF1$^+$ and CD28$^+$ stem-like CD8 T cells increased (Figure 5D and 5E).

As previous studies have shown, antigen presenting cells maintain the stem-like CD8 T cell niche in the TME[31,43]. We have also observed that our fusion protein targets PD-L1 on DCs to

reactivate T cells. Thus, it is possible that stem-like CD8 T cells but not terminally exhausted CD8 T cells were preferentially activated by PDL1xCD3, due to their physiological co-localization with DCs. More importantly, the percentage of antigen specific CD8 T cell in the tumor also increased after PDL1xCD3 treatment (Figure 5F). Thus, PDL1xCD3 may preferentially activate a 'DC-interacting' population of CD8 T cells to establish specific anti-tumor immunity. In addition, we also examined the dynamics of myeloid cells in the TME. The percentage of both macrophages and MDSCs dramatically decreased after treatment since they are considered as 'PD-L1$^+$ targets' (Figure 5G and 5H). Meanwhile, the percentage of DCs also significantly decreased even though they are required for the initiation of the anti-tumor effect (Figure 5I). Notably, the percentage of Tregs was also decreased despite the increase in total CD4 percentage (Figure S5F). Even though the mechanism is still unknown, the expression of PD-L1 on Tregs has been reported, which may be an explanation for this phenomenon[44]. Finally, the dynamics of all these immune populations was restricted to the tumor. PDL1xCD3 treatment did not significantly alter splenic immune cell populations compared to the control group, indicating that the anti-tumor effect was mainly generated in the tumor. Taken together, PDL1xCD3 reshapes the TME to provoke specific anti-tumor immunity.

Co-stimulatory signaling is required for PDL1xCD3 mediated anti-tumor effects

The generation of protective T cell immunity is one of the most desired goals in cancer immunotherapy. However it remains the major hurdle of current tumor cell targeting BiTE therapy. Our data has shown that PDL1xCD3 can target DCs to promote antigen specific T cell immunity. Therefore, we want to further investigate the underlying mechanisms participating in this process. Previous studies have shown that the therapeutic effect of anti-PD-L1 treatment is CD28 dependent which highlights the importance of co-stimulatory signaling in generation of T cell immunity[45,46]. Therefore, we hypothesized that the therapeutic effect of PDL1xCD3 may depend on T cell co-stimulation. To elucidate this hypothesis, we combined anti-CD80/86 antibodies together with PDL1xCD3 treatment (Figure 6A). To our surprise, blocking B7-CD28 co-stimulation completely abolished the therapeutic effect of PDL1xCD3 (Figure 6B). Similar results were also observed when using CTLA4-Ig to block (Figure S6A and S6B). Blocking B7-CD28 interaction also inhibited the generation of antigen specific T cells in the tumor (Figure 6C).

To further determine how co-stimulatory signaling helps DCs generate proper T cell response in the presence of PDL1xCD3, we co-cultured tumor cells or splenic DCs with naïve CD8 T cells in the presence of either ErbxCD3 or PDL1xCD3. Even though targeting tumor cells by PDL1xCD3 induces similar level of $CD25^{+}CD69^{+}$ T cells and IFNγ in the supernatant as targeting dendritic cells (Figure 6D and 6E). The percentage of live T cells was much lower than in DC group. Activation induced cell death (AICD) occurred in tumor-cell-activated T cells treated with either ErbxCD3 or PDL1xCD3, but was greatly reduced in dendritic-cell-activated T cells treated with PDL1xCD3 (Figure 6F). Thus, targeting tumor cell to reactivate T cells may only have transient anti-tumor effect and cannot generate long-lasting effects due to a lack of co-stimulation, increased T cell death and no memory response. Our *in vivo* data also shows that ErbxCD3 treatment group has a lower frequency of intratumoral CD8 T cells compared with the control group, which is consistent with our *in vitro* results here (Figure 5A and 6F). Moreover, when anti-CD80/86 blocking was administered together with PDL1xCD3 in our DC-T cell co-culture, T cell activation was reduced and T cell apoptosis was increased to levels similar to those of tumor-T cell co-cultures (Figure 6D and 6F). This further confirmed that PDL1xCD3 treatment promotes T cell survival through enhancing CD28 costimulation. When cytokines in the supernatant was detected by Cytometric Bead Array (CBA), we observed that the DC-T cell co-culture induced the highest level of IL-2, which is known to support T cell survival and proliferation[47]. However, IL-2 is undetectable in ErbxCD3 group. As expected, the production of IL-2 is also B7-CD28 dependent (Figure 6G). Finally, when TCGA database was analyzed, patients with high level of CD28 expression but not CD8 T cell infiltration have better cumulative survival rate (Figure 6H, 6I and S6C). The level of dendritic cell infiltration and CD80/86 expression correlated with the level of CD28 significantly, which indicates the potential importance of dendritic cell mediated T cell costimulation in anti-cancer immunity (Figure S6D and S6E). In summary, PDL1xCD3 targets dendritic cells to activate antigen specific T cells in a B7-CD28 dependent manner and overcomes the major barrier of conventional BiTE therapy.

Discussion

The implementation of bispecific T-cell engagers to solid tumors has been hampered presumably due to not only short half-life, poor anti-tumor activity and severe toxicity. It raises the possibility that current targeting TAA might not be right strategies. In the presented study, we designed and evaluated the efficacy and safety of a PD-L1 targeting bispecific antibody in syngeneic mouse models. Compared with conventional BiTEs, PDL1xCD3 treatment can generate stronger antigen specific T cell responses *in vivo* to eradicate tumors and establish protective immunity. This immunity depends on preexisting TILs and have memory responses. Mechanistically, targeting a subset of DCs instead of tumor cells with PDL1xCD3 can not only enhance B7-CD28 interaction but also simultaneously block PD-1/PD-L1 checkpoint to establish a proper antigen specific CD8 T cell response to control tumors. Taken together, our study highlights the indispensable role of $Batf3^+$ DCs but not tumor cells in PD-L1 targeting bi-specific antibody therapy to rejuvenate and maintain a durable immune response against cancer.

Even though T cell-redirecting therapies have received advances in patients with hematopoietic malignancies, their safety and efficacy in patients with solid tumors remain very limited. Several anti-CD3 bispecific antibodies have been evaluated in preclinical models, targeting tumor associated antigens like EGFR, Her2 and EpCAM for years[48,49]. Studies using a murine melanoma model have shown that targeting TAAs to redirect T cells to tumor cells fails to generate memory immune responses, and tumors eventually relapse despite the initial control[42]. In our syngeneic mouse study, the TAA-targeting BsAb (ErbxCD3) also activated T cells efficiently to kill tumor cells *in vitro* but had very limited anti-tumor effect *in vivo*. T cell frequency in the tumor decreased after treatment, which indicates that the TME initiates an immune resistance to evade killing. However, PDL1xCD3 treatment could generate a strong anti-tumor effect both *in vitro* and *in vivo*. Thus, these results indicate that targeting PD-L1 to rejuvenate T cells can induce more effective anti-tumor immunity than bridging T cells to tumor cells directly.

One conceptual issue is whether engagement of T cells by tumor cells can sufficiently rejuvenate exhausted T cells. The lack of proper co-stimulatory molecules on tumor cells may resulted in sustained T cell dysfunction[50]. Bispecific antibodies engineered with additional anti-CD28 activity have been reported recently in either a trispecific format or in two separate bispecific antibody combination[25,27]. With additional anti-CD28 signaling, the therapeutic effect is better

than BiTE alone indicating the indispensable role of T cell co-stimulation. However, tumor cells may produce various suppressive factors to restrain T cell re-activation. Therefore, targeting DCs might be a better strategy to rescue those T cells. Furthermore, the cross-linking of either CD3 or CD28 signaling by anti-TAA still depends on the specificity of the tumor associated antigens, which are shared by many normal tissues. Thus, this anti-CD28 strategy also encounters the same 'on-target off-tumor' adverse effects as conventional BiTE therapy. PDL1xCD3 treatment can mainly target DCs *in vivo* instead of tumor cells. Thus, endogenous B7-1&2 from DCs can provide co-stimulatory signaling for T cell activation, which is rarely expressed by tumor cell. Studies have also shown that the therapeutic effect of anti-PD-L1 treatment also depends on dendritic cell and B7 co-stimulation[51]. This study is consistent with a recent study showing the release of CD80 from the CD80&PD-L1 heterodimer, which provides a potential explanation of the mechanism of anti-PD-L1 treatment[52]. In fact, CAR-T and BsAb treatment which targets CD19 for B cell leukemia consistently have better therapeutic effect than for other tumors. This may also be due to B cell lymphoma cell potentially serving as APCs in lymphoid tissues to provide co-stimulation and a local milieu that favors T cell activation.

The undesired 'on-target off-tumor' adverse effect cannot be examined in most animal models (i.e. xenograft) because noncancerous animal tissue does not express the same targeted "human" antigens. Thus, the undesired side effect becomes a major hurdle which limits those antibodies from proceeding beyond phase I clinical trials. The underlying mechanism for *in vivo* immune activation and subsequent cytokine release syndrome (CRS) also remains largely unknown. Studies have shown that monocyte derived IL-6 and IL-1β are the primary source of systemic toxic cytokines and are dispensable for cytotoxic T cell activity [9]. In our study, we also observed an increased level of serum IL-6 at 24 hours post anti-CD3 treatment, which was significantly lower post PDL1xCD3 treatment. No severe body weight loss was observed during and after PDL1xCD3 treatment, which also indicates that targeting PD-L1 to engage anti-CD3 signal can reduce side effects.

Antigen specific T cells play an essential role in establishing specific immunity against cancer. However, in BsAb treatment, all T cells can be reactivated in spite of their TCR specificity. Thus, bystander T cells may get activated more than antigen specific T cells due to their high abundance and relative healthy state inside the TME. Non-specific T cells can generate transient

anti-tumor effects but do not contribute to establish durable and memory T cell responses for distal tumors. Recent studies have shown that the APC niche in the tumor microenvironment maintains a specific subset of stem-like T cell with the expression of TCF1 and CD28[31,43]. Analyses of the TCGA database reveal that CD28 expression highly correlates with DC infiltration in multiple cancers. In addition, our results have also shown that $CD103^+$ cDC1 and preexisting CD8 T cells in the tumor are required for PDL1xCD3 treatment. The percentage of $CD28^+$ and $TCF1^+$ T cells increased after PDL1xCD3 treatment, thus indicating that PDL1xCD3 can activate T cells that are interacting with DCs. The DC-interacting T cells have some unique therapeutic potentials such as better activation due to CD28 expression and interacting with DCs to receive B7 ligation. More importantly, DC-interacting T cells are likely to be antigen specific since DCs are the dominant tumor antigen presenting APC. Our results also showed that antigen-specific T cells increased after treatment. Thus, targeting DCs to rejuvenate T cells for tumor killing may be a better strategy than direct link T cells against tumor cells.

Immune checkpoints are another factor which may limit the anti-tumor effect of BsAb treatment. Studies have demonstrated that blocking PD-1 pathway could enhance the therapeutic effect of anti-CD19 CAR-T[53,54]. There are also several ongoing clinical trials testing the combination of BsAbs with checkpoint blockade [4]. PDL1xCD3 treatment achieved this goal by simultaneously blocking negative signal (PD-L1) and reengaging positive signal (CD3) for sustained T cell activation. PD-L1 may play a dual role for PDL1xCD3 treatment. First, it may act as a target to redirect T cells since tumor tissues have higher level of PD-L1 than other tissues. Our results have shown that intravenously injected PDL1xCD3 preferentially distributes to the tumor. It is known that multiple cells in the TME have high levels of PD-L1 expression including tumor cells, stromal cells, T cells and myeloid cells driven by abundant IFN signaling. Thus, PD-L1 may serve as a potent target for local rejuvenation of T cells in the tumor. Second, the anti-PD-L1 arm of PDL1xCD3 could also block PD-L1/PD-1 pathway to prevent CTLs exhaustion in close proximity during T cell activation. By conditional knocking out PD-L1 on different cells, we demonstrate that PD-L1 on DCs plays an essential role in eliciting therapeutic effect. Intriguingly, $Batf3^+$ DCs are the most efficient APC in cross-presenting tumor antigens to T cells because of their highly professional ability to process antigens[55]. In addition, $Batf3^+$ DCs also express higher levels of PD-L1 than other DCs or tumor cells, leading to be preferentially targeted by our fusion

protein. Since Batf3^{+} DCs are essential for the efficacy of PDL1xCD3, it is possible that PDL1xCD3 brings T cells to this rare but potent APC for their re-activation.

As shown in our data, redirecting T cells to tumor cells for killing only induces a limited immune response. T cells that are activated by CD3 engagement also undergo AICD due to lack of CD28 co-stimulation. IFNγ will not only kill tumor cells but also induce T cell apoptosis [56]. Treatment of high dose ErbxCD3 leads to tumor progression with T cell depletion in the tumor (data not shown). Thus, whether T cell can survive after activation becomes a key factor in determining the therapeutic effect of a BsAb *in vivo*. Treatment with PDL1xCD3, predominantly rejuvenate the T cells interacting with DCs. B7 from DCs may stimulate CD28 signaling for Bcl-XL production to abrogate AICD[23]. We also observed B7 dependent IL-2 production after PDL1xCD3 treatment, which may contribute to T cell expansion and survival. Taken together, these data highlight the importance of targeting DCs to activate T cells. Despite the presented results, we acknowledge limitations of current study. *In vivo* efficacy should also be tested on humanized mouse models in multiple cancers to validate our major conclusions. Other DC-targeting BsAbs should also be compared to PD-L1xCD3 like CD103xCD3 or CD40xCD3 for similar or better anti-tumor immune responses. The combination of PDL1xCD3 with either radiation or anti-CTLA4 should also be tested for the synergistic effect in the future.

In summary, we have revealed not only demonstrates a better anti-tumor results but also proposes a new strategy for BsAb based targeting. Furthermore, we have highlighted the indispensable role of targeting DCs instead of tumor cells for cancer immunotherapy.

Methods

Mice

Female C57BL/6J, BALB/c, *FcγR*$^{-/-}$, *Batf3*$^{-/-}$, *Zbtb46*-Cre and *Lyz2*-Cre mice were purchased from The Jackson Laboratory. Rag1-/- mice on C57BL/6 background were purchased from UT southwestern mice breeding core. *Pdl1*$^{f/f}$ mice were generated in the UT southwestern mice breeding core. *PD-L1*$^{-/-}$ mice were provided by L. Chen (Yale University, New Haven, Connecticut, USA). All mice were maintained under specific pathogen-free conditions. Animal care and experiments were carried out under institutional and National Institutes of Health protocol and guidelines. This study has been approved by the Institutional Animal Care and Use Committee of the University of Texas Southwestern Medical Center.

Cell lines and reagents

B16, MC38 cell lines were purchased from American Type Culture Collection (ATCC). TC-1 cells were kindly provided by Dr. T. C. Wu at John Hopkins University. TUBO was derived from a spontaneous mammary tumor in a BALB/c Neu-Tg mouse. MC38-OVA cells were made by lenti-viral transduction of OVA gene. B16E5, TC1E5, MC38E5 were sorted and sub-cloned after being transduced by lentivirus expressing murine-human chimeric EGFR (full-length of the murine EGFR with six mutated amino acids that are critical for human EGFR binding to Cetuximab). PD-L1 deficient MC38 or B16 cells were generated by CRISPR/Cas9 technology as described by previous study. All cell lines were routinely tested using mycoplasma con-tamination kit (R&D) and cultured in Dulbecco's modified Eagle's medium supplemented with 10% heat-inactivated fetal bovine serum, 100 U/ml penicillin, and 100 U/ml streptomycin under 5% CO2 at 37 °C. Anti-CD4 (GK1.5), anti-NK1.1 (PK136), anti-CD8 (53-5.8), anti-CSF1R (AFS98), anti-CD80 (16-10A1), anti-CD86 (GL-1), and CTLA-Ig mAbs were purchased from BioXCell. FTY720 were purchased from Selleckchem

Flow Cytometry Analysis

Single cell suspensions from either spleen, tumor or *in vitro* co-cultured cells were incubated with anti-FcγIII/II receptor (clone 2.4G2) for 15 minutes to block non-specific binding before staining with the conjugated antibodies. 7-AAD Viability Staining Solution or Fixable Viability Dye eFluor^{TM} 506 was used to exclude dead cells. Foxp3, Ki-67 and TCF1 were stained intracellularly

by using True-Nuclear transcription factor buffer set (BioLegend) following the manufacturer's instructions. To assess the EGFR, PD-L1 binding affinity, EGFR and PD-L1 expressing cells were firstly stained with ErbxCD3, PDL1xCD3 or Control IgG, then PE conjugated donkey anti-human IgG was used as a secondary antibody. To assess the FcγR binding affinity, RAW264.7 cells were first stained with fusion proteins with WT or mutant Fc, then PE conjugated donkey anti-human IgG was used as a secondary antibody. All staining steps were conducted at 4 °C in the dark. BD™ Cytometric Bead Array (CBA) Mouse Th1/Th2/Th17 Kit was used to measure the cytokines in the supernatants from *in vitro* cell culture or mice serum according to the manufacturer's protocol (BD Biosciences). Data were collected on CytoFLEX flow cytometer (Beckman Coulter, Inc) and analyzed by using CytExpert (Beckman Coulter, Inc) or FlowJo (Tree Star Inc., Ashland, OR) software.

Enzyme-Linked ImmunoSorbent Assay (ELISA)

Microtiter plates (Corning Costar) were coated with 2 μg/mL (100 μl/well) capture antibody (AffiniPure Goat Anti-Human IgG, Fcγ fragment specific) overnight at 4 °C. After washing and blocking, diluted tissue lysate from PDL1xCD3 treated mice were added and incubated at 37 °C for 1 hr. After washing, Horseradish Peroxidase (HRP) conjugated Goat Anti-Human IgG (H+L) was added and incubated at 37 °C for 30 minutes. Finally, the plates were visualized by adding 100 μl TMB solution plus 50μL H_2SO_4 and read at 450 nm using the SPECTROstar Nano (BMG LABTECH).

IFN-γ Enzyme-Linked Immunosorbent Spot Assay (ELISPOT)

MC38-OVA ($1x10^6$) tumors were injected subcutaneously on the right flank of C57BL/6. For PDL1xCD3 single treatment, 0.25mg/kg PDL1xCD3 was intraperitoneally given twice on days 10 and 15. 25 days after second treatment, splenocytes from PDL1xCD3 treated and control mice were collected for single-cell suspension preparation. $3x10^5$ splenocytes was seeded in each well with either irradiated MC38-OVA tumor cells ($3x10^4$) or 5 μg/mL SIINFEKL peptide ($OVA_{257-264}$) to stimulate the tumor-specific T cells. After 48 hrs culture, the ELISPOT assay was performed using the IFN-γ ELISPOT kit (BD Bioscience) according to the manufacturer's instructions. IFN-γ spots were enumerated with the CTL-ImmunoSpot® S6 Analyzer (Cellular Technology Limited). For anti-B7-1&2 blocking treatment, 0.25mg/kg PDL1xCD3 was intraperitoneally given twice on days 10 and 15, 200 μg of anti-B7-1&2 was given intraperitoneally on day 10, 13 and 15. $CD45^+$

cells in the tumor were enriched by EasySep™ Biotin Positive Selection Kit II. ELISPOT assay was performed by described above.

Tumor growth and treatment

A total of $1x10^6$ MC38, $3x10^5$ MC38E5, $1x10^6$ MC38OVA, $1x10^6$ TC1E5, $3x10^5$ B16E5, $5x10^5$ TUBOE5, $1x10^6$ MC38-PDL1KO or $5x10^5$ B16F10-PDL1KO cells were inoculated subcutaneously into right dorsal flanks of the mice in 100 μl phosphate buffered saline (PBS). Tumor-bearing mice were randomly grouped into treatment groups when tumors grew to around 80-100mm^3. For PDL1xCD3 treatment, two doses of 0.25mg/kg antibody was intraperitoneally given starting from day 8-10 with 3-4 days interval. For CSF1R, NK1.1, $CD4^+$ and $CD8^+$ T cell depletion, 200 μg of antibodies were intraperitoneally injected 1 day before treatment initiation and then twice a week for 2 weeks. For FTY720 treatment, 20 μg FTY720 was intraperitoneally administrated one day before treatment initiation and then 10 μg every other day for 2 weeks. For anti-B7-1&2 and CTLA-4-Ig treatment, 200μg anti-B7-1, anti-B7-2 or CTLA-4-Ig was administrated on day 10, 13 and 15. For two tumor model, $1x10^6$ MC38 and $1x10^6$ MC38-PDL1KO cells were subcutaneously inoculated into the left and right dorsal flanks of the mice respectively, PDL1xCD3 treatment was given on day 10 and 15. Tumor volumes were measured by the length (a), width (b) and height (h) and calculated as tumor volume = abh/2.

Production of Bispecific Fusion Proteins

Based on the heterodimeric Fc variant KiHss-AkKh platform as previously described, the ScFv fragment of anti-PD-L1 or anti-EGFR was fused with knob variant Fc region, and the anti-CD3 ScFv was fused with hole variant Fc region. PDL1xCD3 and ErbxCD3 was generated by transient co-transfection of two arms of plasmids into FreeStyle™ 293-F cells. The supernatant containing fusion proteins was purified using Protein A affinity chromatography according to the manufacturer's protocol. The heterogeneity and purity were confirmed by SDS-PAGE. Anti-PD-L1 and anti-CD3 homodimer control antibodies were generated and produced in same procedure as described above.

Tissue homogenate preparation

Spleen, kidney, heart, liver and tumor were excised on day 1, 3, 5 after PDL1xCD3 treatment and homogenized in the Cell Lysis Kit (Bio-Rad Laboratories) with the FastPrep-24 5G Homogenizer.

Then centrifuge for 20 minutes at 12000 rpm. Supernatant was collected and stored at -80 °C for ELISA.

Tumor digestion

Tumor tissues were excised and digested with 1 mg/mL Collagenase I (Sigma) and 0.5 mg/mL DNase I (Roche) in the 37°C for 30mins, tumor was then passed through a 70 μm cell strainer to remove large pieces of undigested tumor. Tumor infiltrating cells were washed twice with PBS containing 2 mM EDTA.

Immune cell isolation

$CD8^+$ T cells were isolated from lymph nodes and spleens of naïve C57BL/6J mice with a negative CD8 isolation kit (STEMCELL Technologies) following the manufacturer's instructions. DCs in the spleen and lymph nodes were stained with CD11c and sorted by BD FACSMelody™.

***In Vitro* Co-culture of tumor cells and T Cells**

$3x10^4$ MC38E5-GFP tumor cells and $3x10^5$ naïve CD8 T cells were seeds in 96-well plate with 200 μl of RPMI-1640. A series dilutions of fusion proteins were added to the supernatant. T cell activation, T cell and tumor cell viability and serum cytokines was measured at 24, 48 or 72 hrs after incubation.

TCGA database analyze

Cumulative survival rate in patient with different level of CD28 expression (top 10% vs bottom 10%) and correlation of CD28 expression with CD80&CD86 expression, DCs infiltration were analyzed using TIMER: Tumor IMmune Estimation Resource (https://cistrome.shinyapps.io/timer/)

Statistical analysis

All the data analyses were performed with GraphPad Prism statistical software and shown as mean ± SEM. P value was determined by two-way ANOVA for tumor growth, Log-rank test for survival, Spearman's rho correlation test for correlation or unpaired two-tailed t-tests for other analysis. A value of $p < 0.05$ was considered statistically significant.

Reagent and resource table

525

REAGENT or RESOURCE	SOURCE	IDENTIFIER
Antibodies		
InVivoMAb anti-mouse CD4 (GK1.5)	BioXcell	Cat# BE0003-1
InVivoMAb anti-mouse CD8 (53-5.8)	BioXcell	Cat# BE0223
InVivoMAb anti-mouse NK1.1 (PK136)	BioXcell	Cat# BE0036
InVivoMAb anti-mouse CSF1R (AFS98)	BioXcell	Cat# BE0213
InVivoMAb anti-mouse CD80 (16-10A1)	BioXcell	Cat# BE0024
InVivoMAb anti-mouse CD86 (GL-1)	BioXcell	Cat# BE0025
InVivoMAb recombinant CTLA-4-Ig	BioXcell	Cat# BE0099
Anti-CD45 (Flow cytometry, 30-F11)	BioLegend	Cat# 103126
Anti-CD3 (Flow cytometry, 145-2C11)	BD Biosciences	Cat# 564379
Anti-CD28 (Flow cytometry, 37.51)	BioLegend	Cat# 102109
Anti-CD8 (Flow cytometry, 53-6.7)	BioLegend	Cat# 100730
Anti-CD4 (Flow cytometry, RM4-5)	BD Biosciences	Cat# 550954
Anti-CD25 (Flow cytometry, PC61)	BioLegend	Cat# 102008
Anti-CD69 (Flow cytometry, H1.2F3)	BD Biosciences	Cat# 551113
Anti-CD11b (Flow cytometry, M1/70)	BioLegend	Cat# 101236
Anti-CD11c (Flow cytometry, N418)	BioLegend	Cat# 117306
Anti-CD103 (Flow cytometry, 2E7)	BioLegend	Cat# 121406
Anti-PD-1 (Flow cytometry, 29F.1A12)	BioLegend	Cat# 135224
Anti-TIM3 (Flow cytometry, RMT3-23)	eBioscience	Cat# 25587008
Anti-TCF1 (Flow cytometry, C63D9)	Cell Signaling Technology	Cat# 6444S
Anti-MHCII (Flow cytometry, M5.114.15.2)	eBioscience	Cat# 56-5321-82
Anti-F4/80 (Flow cytometry, REA126)	Miltenyi Biotec	Cat# 130-102-422
Anti-Gr1 (Flow cytometry, RB6-8C5)	BioLegend	Cat# 108440
Anti-B220 (Flow cytometry, RA3-6B2)	BioLegend	Cat# 103226
Anti-NK1.1 (Flow cytometry, PK136)	BD Biosciences	Cat# 552878
Anti-Foxp3 (Flow cytometry, MF-14)	BioLegend	Cat# 126408
Anti-Ki-67 (Flow cytometry, 16A8)	BioLegend	Cat# 652404
Anti-PD-L1 (Flow cytometry, 10F.9G2)	BioLegend	Cat# 124308
Fixable Viability Dye eFluor™ 506	Thermo Fisher	Cat# 65-0866-18
iTAg Tetramer/PE - H-2 Kb OVA (SIINFEKL)	MBL	Cat# TB-5001-1
Anti-FcγIII/II receptor (clone 2.4G2)	BD Biosciences	Cat# 553141
Peroxidase AffiniPure Goat Anti-Human IgG (H+L)	Jackson ImmunoResearch	Cat# 109-035-088
AffiniPure Goat Anti-Human IgG, Fcγ fragment specific	Jackson ImmunoResearch	Cat# 109-005-098
Donkey Anti-Human IgG (H+L)	Jackson ImmunoResearch	Cat# 709-116-149
Annexin V (Flow cytometry)	BioLegend	Cat# 640912

7-AAD Viability Staining Solution (Flow cytometry)	BioLegend	Cat# 420404
Bacterial and Virus Strains		
N/A		
Biological Samples		
N/A		
Chemicals, Peptides, and Recombinant Proteins		
FTY720 (hydrochloride)	Selleckchem	Cat# S5002
TMB Solution (1X)	eBioscience	Cat# 00-4201-56
OVA257-264 (SIINFEKL)	Invivogen	Cat# vac-sin
Dulbecco's Modified Eagle's Medium	Sigma- Aldrich	Cat# D6429
Collagenase type I	Sigma	Cat# C0130
DNase I	Roche	Cat# 11284932001
Critical Commercial Assays		
BD™ Cytometric Bead Array (CBA) Mouse Th1/Th2/Th17 Cytokine Kit	BD Biosciences	Cat# 560485
BD Mouse IFN-γ ELISPOT Sets	BD Biosciences	Cat# 551083
True-Nuclear™ Transcription Factor Buffer Set	BioLegend	Cat# 424401
EasySep™ Mouse CD8+ T Cell Isolation Kit	STEMCELL	Cat# 19853
Deposited Data		
N/A		
Experimental Models: Cell Lines		
B16	ATCC	Cat# CRL-6322
TC-1	Gift from Dr. T.C. Wu	N/A
MC38	ATCC	N/A
FreeStyle™ 293-F	Thermo Fisher	Cat# R79007
TUBO	Rovero et al., 2000	N/A
Experimental Models: Organisms/Strains		
C57BL/6J	Jackson Laboratory	Cat# 000664
BALB/c	Jackson Laboratory	Cat# 000651
B6.129S7-Rag1tm1Mom/J	UTSW breeding Core	
B6;129P2-Fcer1gtm1Rav/J	Jackson Laboratory	Cat# 002847
B6.129S(C)-Batf3tm1Kmm/J	Jackson Laboratory	Cat# 013755
PD-L1$^{-/-}$	Gift from Dr. Lieping Chen	N/A
Zbtb46^{Cre}Cd274$^{flox/flox}$	This paper	N/A
Lyz2^{Cre}Cd274$^{flox/flox}$	This paper	N/A
Oligonucleotides		
N/A		
Recombinant DNA		
Plasmid: pEE6.4-17A2-Fc6	This paper	N/A
Plasmid: pEE6.4-Erb-Fc9	This paper	N/A
Plasmid: pEE6.4-PD-L1-Fc9	This paper	N/A

Software and Algorithms		
GraphPad Prism software 7.0	GraphPad Software, Inc.	https://graphpad.com/scientific-software/prism/
CTL-ImmunoSpot® S6 Analyzer	Cellular Technology Limited	http://www.immunospot.com/ImmunoSpot-analyzers
CytExpert	Beckman Coulter, Inc	https://www.beckman.com/coulter-flow-cytometers/cytoflex/cytexpert
BD FACSChorus™ Software	BD Biosciences	https://www.bdbiosciences.com/en-us/instruments/research-instruments/research-software/flow-cytometry-acquisition/facschorus-software
FlowJo	Tree Star Inc.	https://www.flowjo.com/solutions/flowjo
Image Lab™ Software	Bio-Rad	http://www.bio-rad.com/en-us/category/image-analysis-software
Other		
TIMER: Tumor IMmune Estimation Resource	Li et al., 2017	https://cistrome.shinyapps.io/timer/

526

References

1 Staerz, U. D., Kanagawa, O. & Bevan, M. J. Hybrid antibodies can target sites for attack by T cells. *Nature* **314**, 628-631, doi:10.1038/314628a0 (1985).

2 Garber, K. Bispecific antibodies rise again. *Nature reviews. Drug discovery* **13**, 799-801, doi:10.1038/nrd4478 (2014).

3 Baeuerle, P. A. & Reinhardt, C. Bispecific T-cell engaging antibodies for cancer therapy. *Cancer research* **69**, 4941-4944, doi:10.1158/0008-5472.CAN-09-0547 (2009).

4 Trabolsi, A., Arumov, A. & Schatz, J. H. T Cell-Activating Bispecific Antibodies in Cancer Therapy. *Journal of immunology* **203**, 585-592, doi:10.4049/jimmunol.1900496 (2019).

5 Bargou, R. *et al.* Tumor regression in cancer patients by very low doses of a T cell-engaging antibody. *Science* **321**, 974-977, doi:10.1126/science.1158545 (2008).

6 Topp, M. S. *et al.* Safety and activity of blinatumomab for adult patients with relapsed or refractory B-precursor acute lymphoblastic leukaemia: a multicentre, single-arm, phase 2 study. *The Lancet. Oncology* **16**, 57-66, doi:10.1016/S1470-2045(14)71170-2 (2015).

7 Maude, S. L., Barrett, D., Teachey, D. T. & Grupp, S. A. Managing cytokine release syndrome associated with novel T cell-engaging therapies. *Cancer journal* **20**, 119-122, doi:10.1097/PPO.0000000000000035 (2014).

8 Topp, M. S. *et al.* Phase II trial of the anti-CD19 bispecific T cell-engager blinatumomab shows hematologic and molecular remissions in patients with relapsed or refractory B-precursor acute lymphoblastic leukemia. *Journal of clinical oncology : official journal of the American Society of Clinical Oncology* **32**, 4134-4140, doi:10.1200/JCO.2014.56.3247 (2014).

9 Li, J. *et al.* CD3 bispecific antibody-induced cytokine release is dispensable for cytotoxic T cell activity. *Science translational medicine* **11**, doi:10.1126/scitranslmed.aax8861 (2019).

10 Reusch, U. *et al.* Anti-CD3 x anti-epidermal growth factor receptor (EGFR) bispecific antibody redirects T-cell cytolytic activity to EGFR-positive cancers in vitro and in an animal model. *Clinical cancer research : an official journal of the American Association for Cancer Research* **12**, 183-190, doi:10.1158/1078-0432.CCR-05-1855 (2006).

11 Cioffi, M., Dorado, J., Baeuerle, P. A. & Heeschen, C. EpCAM/CD3-Bispecific T-cell engaging antibody MT110 eliminates primary human pancreatic cancer stem cells. *Clinical cancer research : an official journal of the American Association for Cancer Research* **18**, 465-474, doi:10.1158/1078-0432.CCR-11-1270 (2012).

12 Han, H. *et al.* Bispecific anti-CD3 x anti-HER2 antibody mediates T cell cytolytic activity to HER2-positive colorectal cancer in vitro and in vivo. *International journal of oncology* **45**, 2446-2454, doi:10.3892/ijo.2014.2663 (2014).

13 of, I. *et al.* A multicenter phase 1 study of solitomab (MT110, AMG 110), a bispecific EpCAM/CD3 T-cell engager (BiTE(R)) antibody construct, in patients with refractory solid tumors. *Oncoimmunology* **7**, e1450710, doi:10.1080/2162402X.2018.1450710 (2018).

14 Kebenko, M. *et al.* A multicenter phase 1 study of solitomab (MT110, AMG 110), a bispecific EpCAM/CD3 T-cell engager (BiTE(R)) antibody construct, in patients with refractory solid tumors. *Oncoimmunology* **7**, e1450710, doi:10.1080/2162402X.2018.1450710 (2018).

15 Lutterbuese, R. *et al.* T cell-engaging BiTE antibodies specific for EGFR potently eliminate KRAS- and BRAF-mutated colorectal cancer cells. *Proceedings of the National Academy of Sciences of the United States of America* **107**, 12605-12610, doi:10.1073/pnas.1000976107 (2010).
16 van Panhuys, N. TCR Signal Strength Alters T-DC Activation and Interaction Times and Directs the Outcome of Differentiation. *Frontiers in immunology* **7**, 6, doi:10.3389/fimmu.2016.00006 (2016).
17 Chai, J. G. & Lechler, R. I. Immobilized anti-CD3 mAb induces anergy in murine naive and memory CD4+ T cells in vitro. *International immunology* **9**, 935-944, doi:10.1093/intimm/9.7.935 (1997).
18 Harding, F. A., McArthur, J. G., Gross, J. A., Raulet, D. H. & Allison, J. P. CD28-mediated signalling co-stimulates murine T cells and prevents induction of anergy in T-cell clones. *Nature* **356**, 607-609, doi:10.1038/356607a0 (1992).
19 Green, D. R., Droin, N. & Pinkoski, M. Activation-induced cell death in T cells. *Immunological reviews* **193**, 70-81, doi:10.1034/j.1600-065x.2003.00051.x (2003).
20 Curtsinger, J. M. & Mescher, M. F. Inflammatory cytokines as a third signal for T cell activation. *Current opinion in immunology* **22**, 333-340, doi:10.1016/j.coi.2010.02.013 (2010).
21 Kalos, M. *et al.* T cells with chimeric antigen receptors have potent antitumor effects and can establish memory in patients with advanced leukemia. *Science translational medicine* **3**, 95ra73, doi:10.1126/scitranslmed.3002842 (2011).
22 MacKay, M. *et al.* The therapeutic landscape for cells engineered with chimeric antigen receptors. *Nature biotechnology* **38**, 233-244, doi:10.1038/s41587-019-0329-2 (2020).
23 Boise, L. H. *et al.* CD28 costimulation can promote T cell survival by enhancing the expression of Bcl-XL. *Immunity* **3**, 87-98, doi:10.1016/1074-7613(95)90161-2 (1995).
24 Garfall, A. L. & June, C. H. Trispecific antibodies offer a third way forward for anticancer immunotherapy. *Nature* **575**, 450-451, doi:10.1038/d41586-019-03495-3 (2019).
25 Skokos, D. *et al.* A class of costimulatory CD28-bispecific antibodies that enhance the antitumor activity of CD3-bispecific antibodies. *Science translational medicine* **12**, doi:10.1126/scitranslmed.aaw7888 (2020).
26 Suntharalingam, G. *et al.* Cytokine storm in a phase 1 trial of the anti-CD28 monoclonal antibody TGN1412. *The New England journal of medicine* **355**, 1018-1028, doi:10.1056/NEJMoa063842 (2006).
27 Wu, L. *et al.* Trispecific antibodies enhance the therapeutic efficacy of tumor-directed T cells through T cell receptor co-stimulation. *Nature Cancer* **1**, 86-98, doi:10.1038/s43018-019-0004-z (2020).
28 Binnewies, M. *et al.* Understanding the tumor immune microenvironment (TIME) for effective therapy. *Nature medicine* **24**, 541-550, doi:10.1038/s41591-018-0014-x (2018).
29 Choi, B. D. *et al.* Human regulatory T cells kill tumor cells through granzyme-dependent cytotoxicity upon retargeting with a bispecific antibody. *Cancer immunology research* **1**, 163, doi:10.1158/2326-6066.CIR-13-0049 (2013).
30 Knutson, K. L. & Disis, M. L. Tumor antigen-specific T helper cells in cancer immunity and immunotherapy. *Cancer immunology, immunotherapy : CII* **54**, 721-728, doi:10.1007/s00262-004-0653-2 (2005).

31 Jansen, C. S. *et al.* An intra-tumoral niche maintains and differentiates stem-like CD8 T cells. *Nature* **576**, 465-470, doi:10.1038/s41586-019-1836-5 (2019).

32 Zou, W., Wolchok, J. D. & Chen, L. PD-L1 (B7-H1) and PD-1 pathway blockade for cancer therapy: Mechanisms, response biomarkers, and combinations. *Science translational medicine* **8**, 328rv324, doi:10.1126/scitranslmed.aad7118 (2016).

33 Lin, H. *et al.* Host expression of PD-L1 determines efficacy of PD-L1 pathway blockade-mediated tumor regression. *The Journal of clinical investigation* **128**, 805-815, doi:10.1172/JCI96113 (2018).

34 Tang, H. *et al.* PD-L1 on host cells is essential for PD-L1 blockade–mediated tumor regression. *The Journal of clinical investigation* **128**, 580-588, doi:10.1172/JCI96061 (2018).

35 Garcia-Diaz, A. *et al.* Interferon Receptor Signaling Pathways Regulating PD-L1 and PD-L2 Expression. *Cell reports* **19**, 1189-1201, doi:10.1016/j.celrep.2017.04.031 (2017).

36 Kohnke, T., Krupka, C., Tischer, J., Knosel, T. & Subklewe, M. Increase of PD-L1 expressing B-precursor ALL cells in a patient resistant to the CD19/CD3-bispecific T cell engager antibody blinatumomab. *Journal of hematology & oncology* **8**, 111, doi:10.1186/s13045-015-0213-6 (2015).

37 Kobold, S., Pantelyushin, S., Rataj, F. & Vom Berg, J. Rationale for Combining Bispecific T Cell Activating Antibodies With Checkpoint Blockade for Cancer Therapy. *Frontiers in oncology* **8**, 285, doi:10.3389/fonc.2018.00285 (2018).

38 Schlothauer, T. *et al.* Novel human IgG1 and IgG4 Fc-engineered antibodies with completely abolished immune effector functions. *Protein engineering, design & selection : PEDS* **29**, 457-466, doi:10.1093/protein/gzw040 (2016).

39 Wei, H. *et al.* Structural basis of a novel heterodimeric Fc for bispecific antibody production. *Oncotarget* **8**, 51037-51049, doi:10.18632/oncotarget.17558 (2017).

40 Qiao, J. *et al.* Targeting Tumors with IL-10 Prevents Dendritic Cell-Mediated CD8(+) T Cell Apoptosis. *Cancer cell* **35**, 901-915 e904, doi:10.1016/j.ccell.2019.05.005 (2019).

41 Wallberg, M. *et al.* Anti-CD3 treatment up-regulates programmed cell death protein-1 expression on activated effector T cells and severely impairs their inflammatory capacity. *Immunology* **151**, 248-260, doi:10.1111/imm.12729 (2017).

42 Benonisson, H. *et al.* CD3-Bispecific Antibody Therapy Turns Solid Tumors into Inflammatory Sites but Does Not Install Protective Memory. *Molecular cancer therapeutics* **18**, 312-322, doi:10.1158/1535-7163.MCT-18-0679 (2019).

43 Sade-Feldman, M. *et al.* Defining T Cell States Associated with Response to Checkpoint Immunotherapy in Melanoma. *Cell* **175**, 998-1013 e1020, doi:10.1016/j.cell.2018.10.038 (2018).

44 Diskin, B. *et al.* PD-L1 engagement on T cells promotes self-tolerance and suppression of neighboring macrophages and effector T cells in cancer. *Nature immunology* **21**, 442-454, doi:10.1038/s41590-020-0620-x (2020).

45 Hui, E. *et al.* T cell costimulatory receptor CD28 is a primary target for PD-1-mediated inhibition. *Science* **355**, 1428-1433, doi:10.1126/science.aaf1292 (2017).

46 Kamphorst, A. O. *et al.* Rescue of exhausted CD8 T cells by PD-1-targeted therapies is CD28-dependent. *Science* **355**, 1423-1427, doi:10.1126/science.aaf0683 (2017).

47 Kelly, E., Won, A., Refaeli, Y. & Van Parijs, L. IL-2 and related cytokines can promote T cell survival by activating AKT. *Journal of immunology* **168**, 597-603, doi:10.4049/jimmunol.168.2.597 (2002).

48 Heiss, M. M. *et al.* The trifunctional antibody catumaxomab for the treatment of malignant ascites due to epithelial cancer: Results of a prospective randomized phase II/III trial. *International journal of cancer* **127**, 2209-2221, doi:10.1002/ijc.25423 (2010).
49 Kiewe, P. *et al.* Phase I trial of the trifunctional anti-HER2 x anti-CD3 antibody ertumaxomab in metastatic breast cancer. *Clinical cancer research : an official journal of the American Association for Cancer Research* **12**, 3085-3091, doi:10.1158/1078-0432.CCR-05-2436 (2006).
50 Schildberg, F. A., Klein, S. R., Freeman, G. J. & Sharpe, A. H. Coinhibitory Pathways in the B7-CD28 Ligand-Receptor Family. *Immunity* **44**, 955-972, doi:10.1016/j.immuni.2016.05.002 (2016).
51 Mayoux, M. *et al.* Dendritic cells dictate responses to PD-L1 blockade cancer immunotherapy. *Science translational medicine* **12**, doi:10.1126/scitranslmed.aav7431 (2020).
52 Zhao, Y. *et al.* PD-L1:CD80 Cis-Heterodimer Triggers the Co-stimulatory Receptor CD28 While Repressing the Inhibitory PD-1 and CTLA-4 Pathways. *Immunity* **51**, 1059-1073 e1059, doi:10.1016/j.immuni.2019.11.003 (2019).
53 Rafiq, S. *et al.* Targeted delivery of a PD-1-blocking scFv by CAR-T cells enhances anti-tumor efficacy in vivo. *Nature biotechnology* **36**, 847-856, doi:10.1038/nbt.4195 (2018).
54 Hill, B. T., Roberts, Z. J., Xue, A., Rossi, J. M. & Smith, M. R. Rapid tumor regression from PD-1 inhibition after anti-CD19 chimeric antigen receptor T-cell therapy in refractory diffuse large B-cell lymphoma. *Bone marrow transplantation*, doi:10.1038/s41409-019-0657-3 (2019).
55 del Rio, M. L., Bernhardt, G., Rodriguez-Barbosa, J. I. & Forster, R. Development and functional specialization of CD103+ dendritic cells. *Immunological reviews* **234**, 268-281, doi:10.1111/j.0105-2896.2009.00874.x (2010).
56 Refaeli, Y., Van Parijs, L., Alexander, S. I. & Abbas, A. K. Interferon gamma is required for activation-induced death of T lymphocytes. *The Journal of experimental medicine* **196**, 999-1005, doi:10.1084/jem.20020666 (2002).

Acknowledgments

We thank the Institutional Animal Care and Use Committee Animal Resources Center, and Animal Research Center. Y.-X.F. holds the Mary Nell and Ralph B. Rogers Professorship in Immunology. This work was supported by Cancer Prevention and Research Institute of Texas (CPRIT) grant RR150072 given to Y.-X.F. We also thank Yong Liang, Xuezhi Cao, Zhenhua Ren, Anli Zhang, Chunbo Dong, Casey Moore, Jian Qiao and Benjamin Moon for providing experiment materials and helpful discussions.

Author contributions

Conceptualization, L.L. and Y.-X.F.; Methodology, L.L. and Y.-X.F.; Investigation, L.L., J.C., Z.L. and J.B.; Writing - Original Draft, L.L.; Writing-Review & Editing, E.H., Y.-X.F.; Funding Acquisition, Y.-X.F.; Resources, C.H. and C.L.; Supervision, Y.-X.F.

Declaration of Interests

The authors declare no competing interests.

Figures and Figure Legends

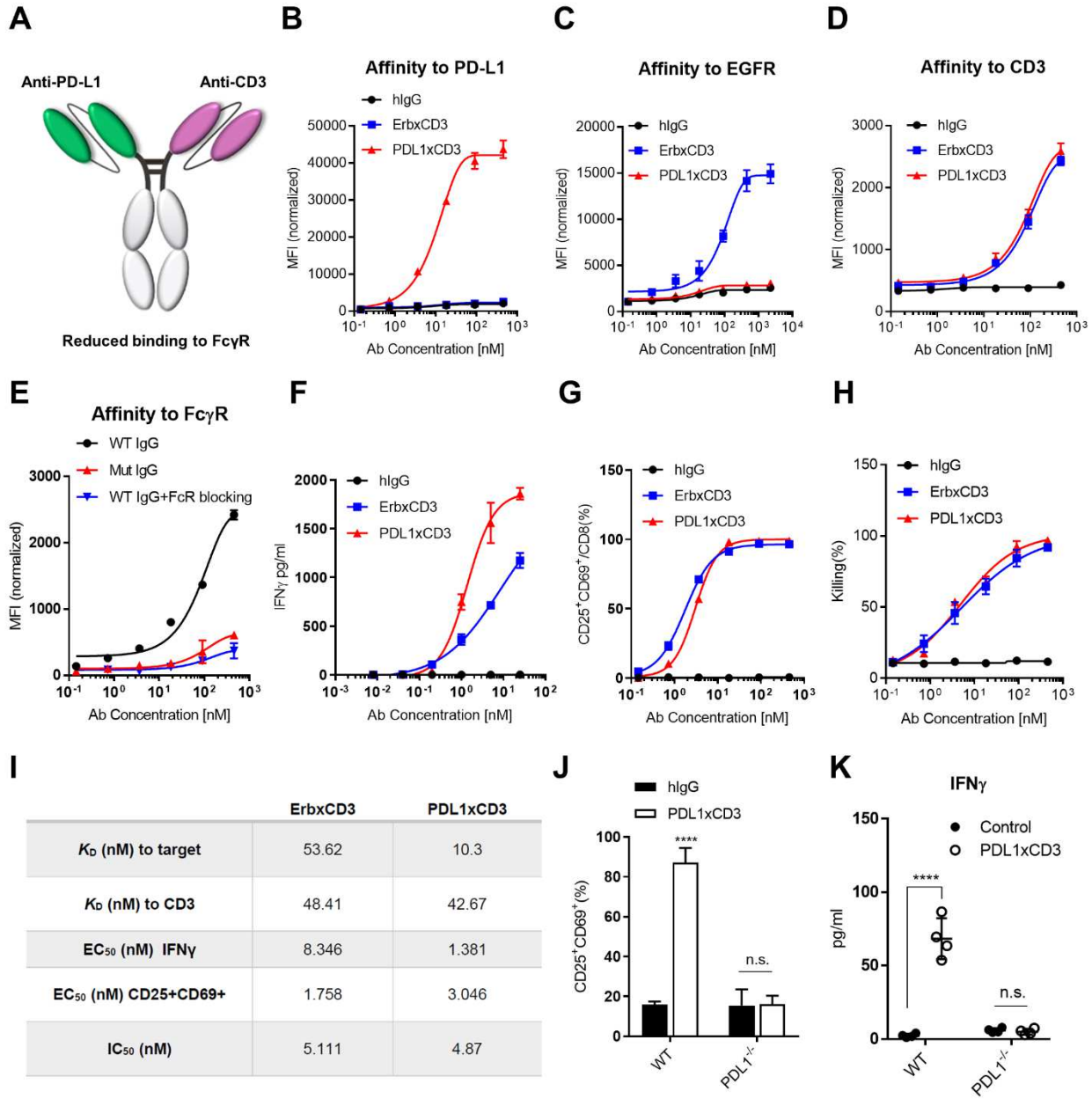

	ErbxCD3	PDL1xCD3
K_D (nM) to target	53.62	10.3
K_D (nM) to CD3	48.41	42.67
EC_{50} (nM) IFNγ	8.346	1.381
EC_{50} (nM) CD25+CD69+	1.758	3.046
IC_{50} (nM)	5.111	4.87

Figure 1. PDL1xCD3 targets PD-L1 to activate T cells in *vitro*.

(A) Schematic structure of PDL1xCD3 bispecific antibody. PDL1xCD3 is composed of a single-chain variable fragment (ScFv) to PD-L1 and a ScFv to murine CD3ε, fused to a mutant human IgG1. (B) Binding of PDL1xCD3 to PD-L1 on MC38 cells overexpressing PD-L1. Cells were incubated with serial dilutions of PDL1xCD3, ErbxCD3, or human IgG control, followed by a

fluorophore-conjugated anti-human IgG secondary antibody. Flow cytometry measured mean fluorescence intensity (MFI) (n=3). (C) Binding of PDL1xCD3 to EGFR on MC38 cells ectopically expressing chimeric EGFR (MC38E5). Cells were incubated with serial dilutions of PDL1xCD3, ErbxCD3, or human IgG control, followed by a fluorophore-conjugated anti-human IgG secondary antibody. Flow cytometry measured MFI (n=3). (D) Binding of PDL1xCD3 to CD3ε on CD8 T cells purified from mouse spleen. Cells were incubated with serial dilutions of PDL1xCD3, ErbxCD3, or human IgG control, followed by a fluorophore-conjugated anti-human IgG secondary antibody. Flow cytometry measured MFI (n=3). (E) Binding of PDL1xCD3 to FcγR on RAW 264.7 cells. Cells were incubated with serial dilutions of WT IgG fusion protein, mutant IgG fusion protein, or WT IgG fusion protein with anti- FcγR, followed by a fluorophore-conjugated anti-human IgG secondary antibody. Flow cytometry measured MFI (n=3). (F-H) MC38E5-GFP cells ($3x10^4$) and purified splenic CD8 T cells ($3x10^5$) were co-cultured with serial dilutions of PDL1xCD3, ErbxCD3, or human IgG control. IFNγ in the supernatant was detected by cytokine beads array (CBA) (F). CD25 and CD69 expression on T cells were detected by flow cytometry (G). GFP^+ $7AAD^-$ tumor cells were detected by flow cytometry (H). (I) Summary of the K_D, EC50 and IC50 of both antibodies. (J-K) Co-culture assay was performed with WT or PD-L1 KO MC38 as in (F), T cell activation (J) and IFNγ in the supernatant (K) were detected respectively. Data are shown as means ± SD, non-linear best fits for (B-H) and two-tailed unpaired t test for (J-K), ****$P \leq 0.0001$. All experiments were repeated twice.

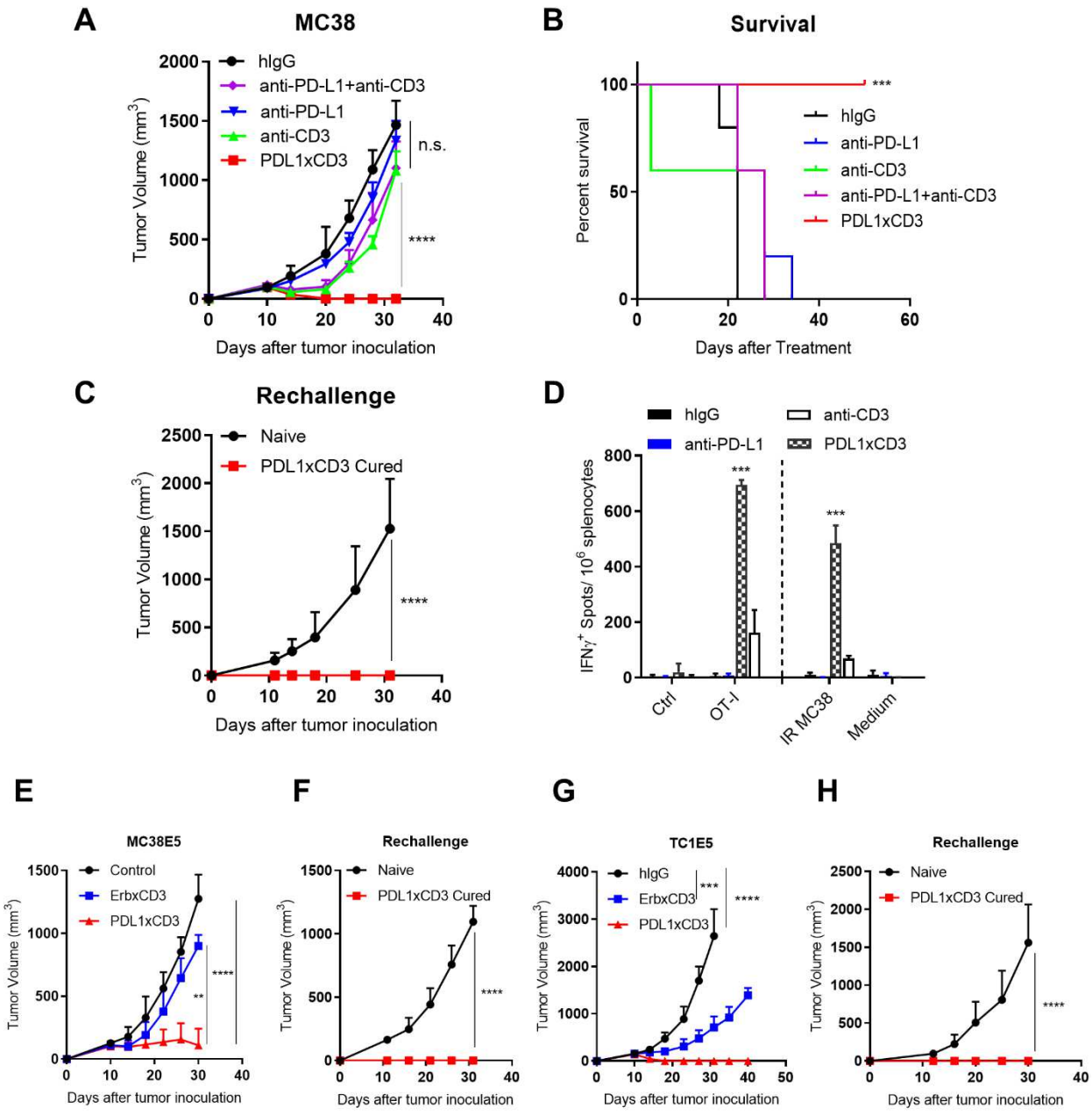

Figure 2. PDL1xCD3 generates superior anti-tumor effect than TAA-targeting BiTE *in vivo*.

(A-C) C57BL/6J mice were subcutaneously inoculated with $1x10^6$ MC38 tumor cells and treated with 0.25 mg/kg of fusion proteins twice on day 10 and 15. Tumor volume (A) and percentage of survival (B) was shown. (C) 50 days after PDL1xCD3 treatment, cured mice were re-challenged with $1x10^7$ MC38 tumor cells. (D) C57BL/6J mice were subcutaneously inoculated with $1x10^6$ MC38OVA tumor cells and treated as in panel A. 25 days after treatment, antigen specific T cells

were detected by Elispot assay with splenocytes. (E-F) C57BL/6J mice were subcutaneously inoculated with $3x10^5$ MC38E5 tumor cells and treated with 0.25 mg/kg of fusion proteins twice on day 10 and 15. (E) Tumor volume was measured twice per week. (F) 60 days post treatment, tumor free mice were re-challenged with $3x10^6$ tumor cells. (G-H) C57BL/6J mice were subcutaneously inoculated with $1x10^6$ TC1E5 tumor cells and treated with 0.25 mg/kg of fusion proteins twice on day 10 and 15. (G) Tumor volume was measured twice per week. (H) 60 days post treatment, tumor free mice were re-challenged with $1x10^7$ tumor cells. Data were shown as mean ± SEM (n=5) from two independent experiments. Statistical analysis was performed by two-way ANOVA and Log-rank test (B), **P ≤ 0.01, ***P ≤ 0.001, and ****P ≤ 0.0001.

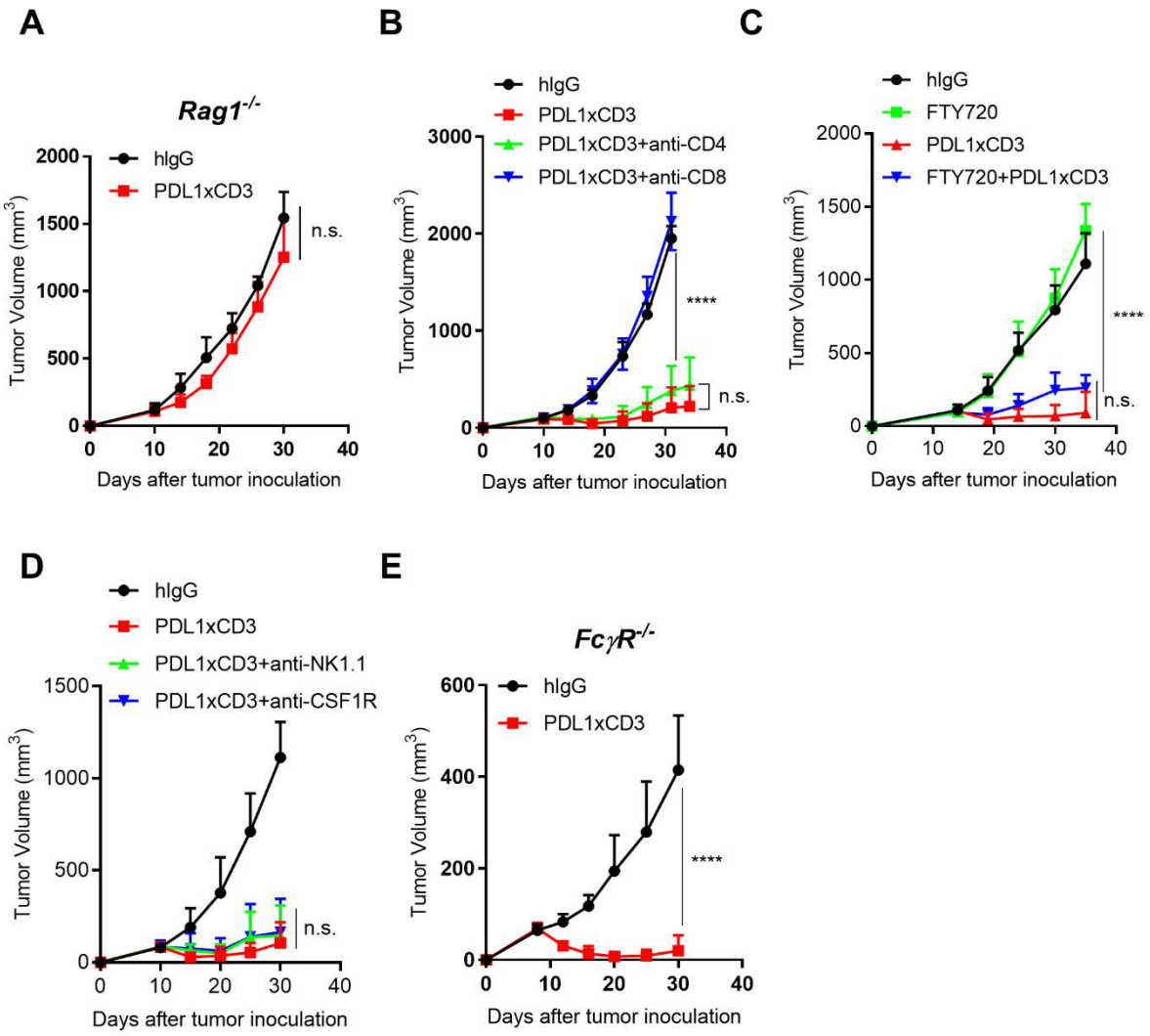

Figure 3. Pre-existing CD8 T cells are required for PDL1xCD3 treatment.

(A) *Rag1*$^{-/-}$ mice were inoculated with 1x10^6 MC38 tumor cells and treated with PDL1xCD3 (0.25 mg/kg on day 10 and 15). (B) C57BL/6 mice were inoculated with 1x10^6 MC38 tumor cells and treated with PDL1xCD3 (0.25 mg/kg on day 10 and 15). 200µg anti-CD8 or anti-CD4 was administrated one day before treatment initiation and then twice a week for 2 weeks. (C) C57BL/6 mice were inoculated with 1x10^6 MC38 tumor cells and treated with PDL1xCD3 (0.25 mg/kg on day 14 and 18). 20µg FTY720 was administrated one day before treatment initiation and then 10µg every other day for 2 weeks. (D) C57BL/6 mice were inoculated with 1x10^6 MC38 tumor cells

and treated with PDL1xCD3 (0.25 mg/kg on day 10 and 15). 200µg anti-NK1.1 or anti-CSF1R was administrated one day before treatment initiation and then twice a week for 2 weeks. (E) *Fcγ*$R^{-/-}$ mice were inoculated with $1x10^6$ MC38 tumor cells and treated with PDL1xCD3 (0.25 mg/kg on day 8 and 12). Data were shown as mean ± SEM (n=5) from two independent experiments. Statistical analysis was performed by two-way ANOVA, ****$P \leq 0.0001$.

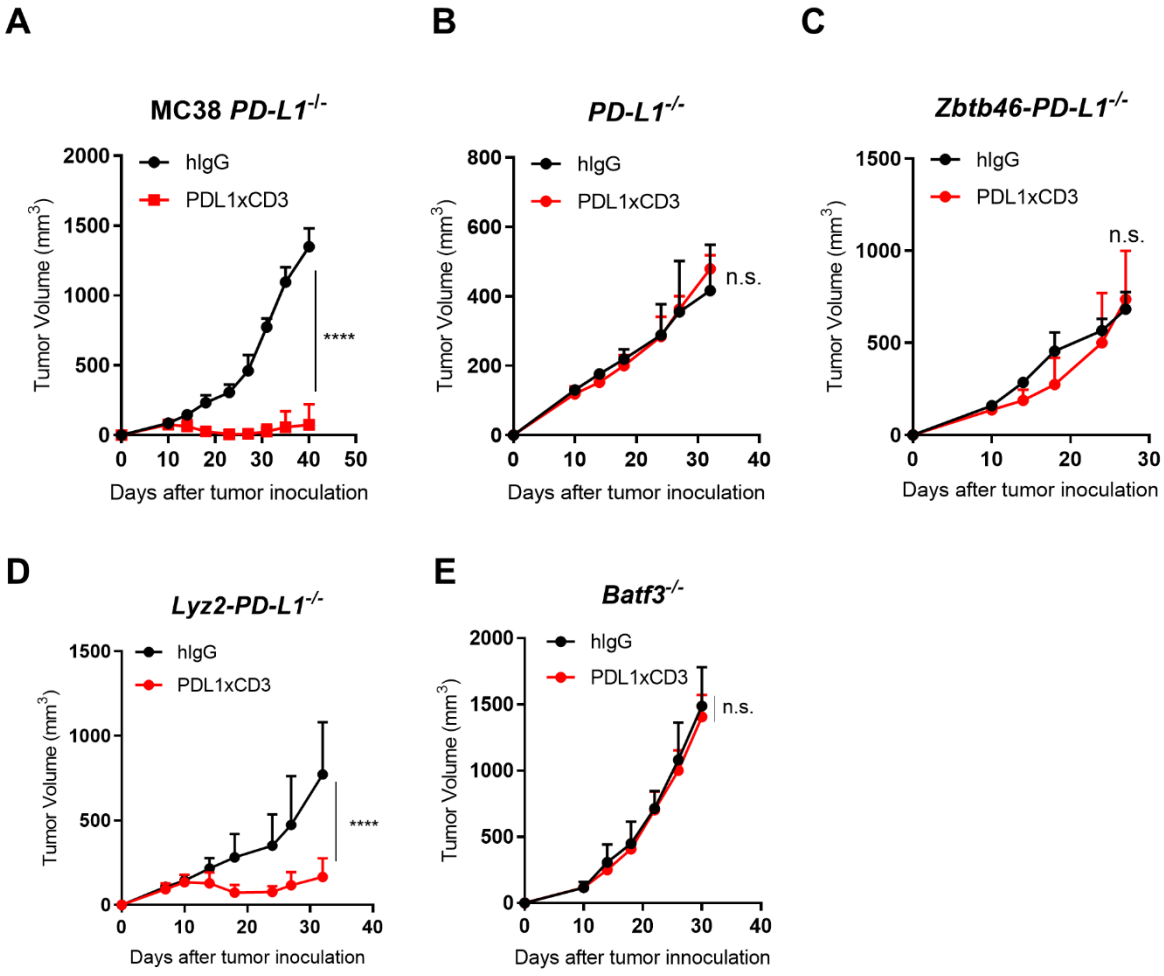

761

762 **Figure 4. PD-L1 on dendritic cells is essential for the anti-tumor effect of PDL1xCD3.**

763 (A) C57BL/6J mice (n=5) were subcutaneously inoculated with 1x10^6 MC38-PDL1$^{-/-}$ tumor cells
764 and treated with 0.25 mg/kg of fusion proteins twice on day 10 and 15. (B) PDL1$^{-/-}$ mice (n=5)
765 were subcutaneously inoculated with 1x10^6 MC38 tumor cells and treated with 0.25 mg/kg of
766 fusion proteins twice on day 10 and 15. (C) *Zbtb46*-Cre-*PD-L1* $^{f/f}$ mice (n=5) were subcutaneously
767 inoculated with 1x10^6 MC38 tumor cells and treated with 0.25 mg/kg of fusion proteins twice on
768 day 10 and 15. (D) *Lyz2*-Cre-*PD-L1* $^{f/f}$ mice (n=5) were subcutaneously inoculated with 1x10^6
769 MC38 tumor cells and treated with 0.25 mg/kg of fusion proteins twice on day 10 and 15. (E)

770 *Batf3*$^{-/-}$ mice were inoculated with 1x10^{6} MC38 tumor cells and treated with PDL1xCD3 (0.25
771 mg/kg on day 10 and 15). Data were shown as mean ± SEM from two independent experiments.
772 Statistical analysis was performed by two-way ANOVA, ****P ≤ 0.0001.

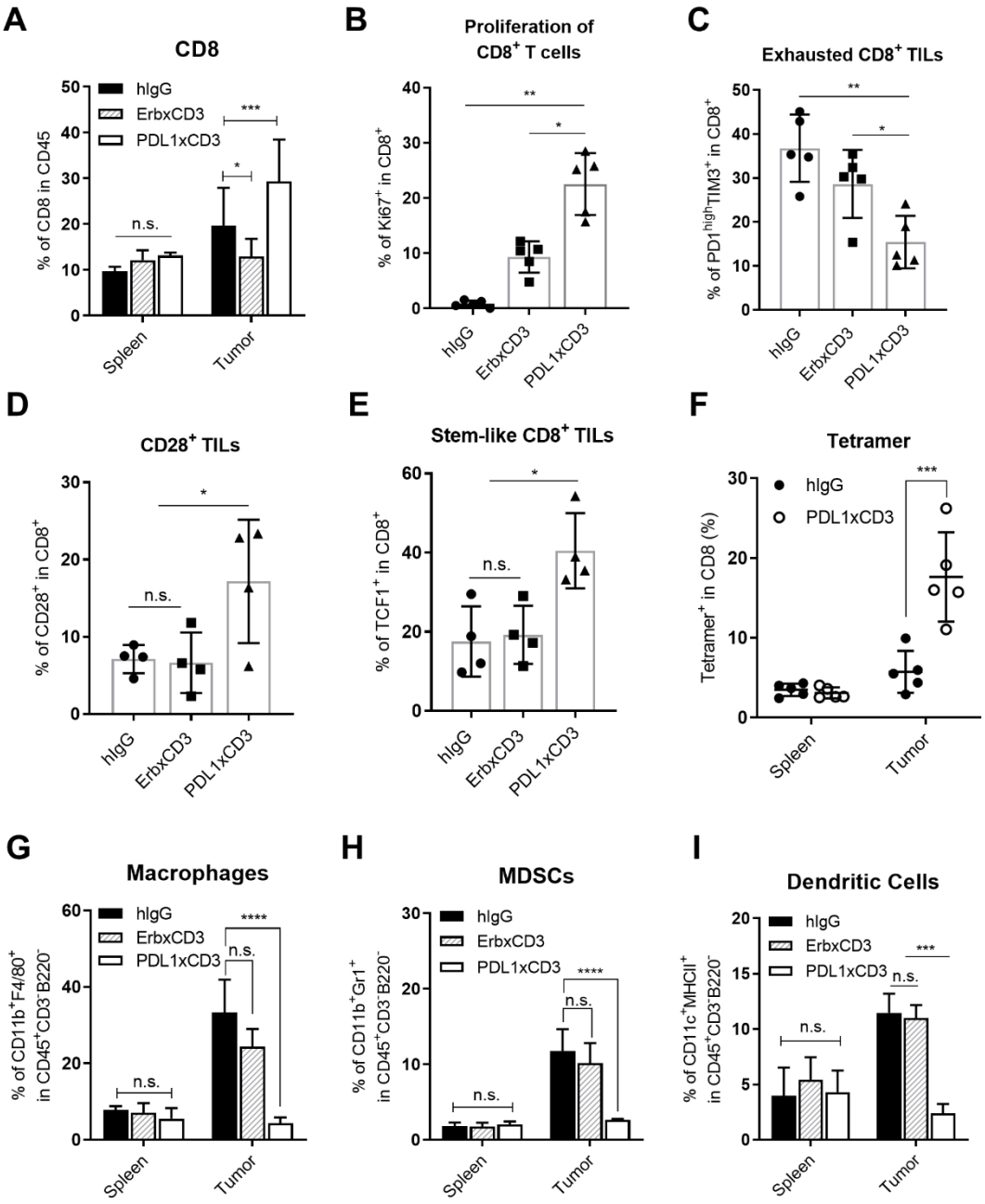

Figure 5. PDL1xCD3 reshapes a distinct immunophenotypic signature in tumor-bearing mice.

C57BL/6J mice (n=5) were subcutaneously inoculated with $1x10^6$ MC38-OVA tumor cells and treated with 0.25 mg/kg of fusion proteins. Flow cytometry analysis was performed with splenocytes and dissociated tumor samples for the percentage of CD8 T cells (A), Ki-67$^+$ CD8 T cells (B), PD-1^{high} TIM-3$^+$ CD8 T cells (C), CD28$^+$ CD8 T cells (D), TCF1$^+$ CD8 T cells (E),

780 tetramer^{+} cells (F), F4/80^{+}CD11b^{+} cells (G), Gr1^{+}CD11b^{+} cells (H), MHC-II^{+}CD11c^{+} cells (I).
781 Representative result from two independent experiments were shown as mean ± SEM (n=5).
782 Statistical analysis was performed by two-tailed unpaired t test, *P ≤ 0.05, **P ≤ 0.01, ***P ≤
783 0.001, and ****P ≤ 0.0001.

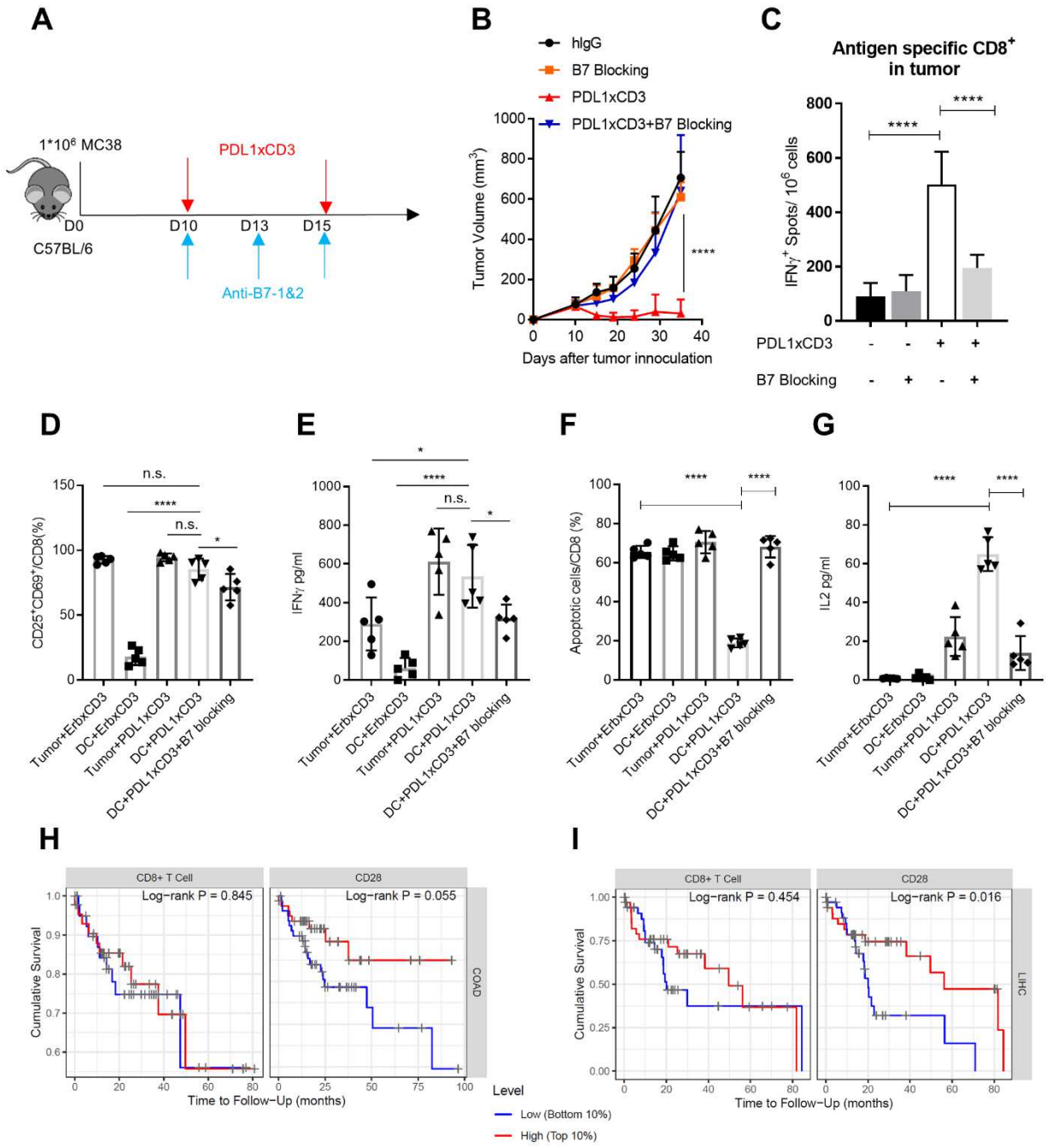

Figure 6. Co-stimulatory signaling is required for PDL1xCD3 mediated anti-tumor effects.

(A-C) C57BL/6J mice were inoculated with $1x10^6$ MC38 tumor cells and treated with PDL1xCD3 (0.25 mg/kg on day 10 and 15), 200 μg anti-B7-1 and anti-B7-2 were administrated on day 10, 13 and 15. Experimental design (A). Tumor growth curve (B) and IFNγ-producing antigen specific CD8 T cells (C) were shown. (D-G) CD8 T cells were co-cultured with either tumor cells or

dendritic cells in the presence of fusion proteins. T cell activation (D), supernatant IFNγ (E), apoptotic T cells (F) and supernatant IL2 (G) were measured by flow cytometry and CBA. (H-I) Cumulative survival in colorectal adenocarcinoma (COAD) and liver hepatocellular carcinoma (LIHC) patients according to CD8 infiltration and CD28 level in TCGA database. Representative result from two independent experiments were shown as mean ± SEM (n=5). Statistical analysis was performed by two-tailed unpaired t test (C-G), two-way ANOVA (B) and Log-rank test (H-I) *P ≤ 0.05, ****P ≤ 0.0001.

Figures

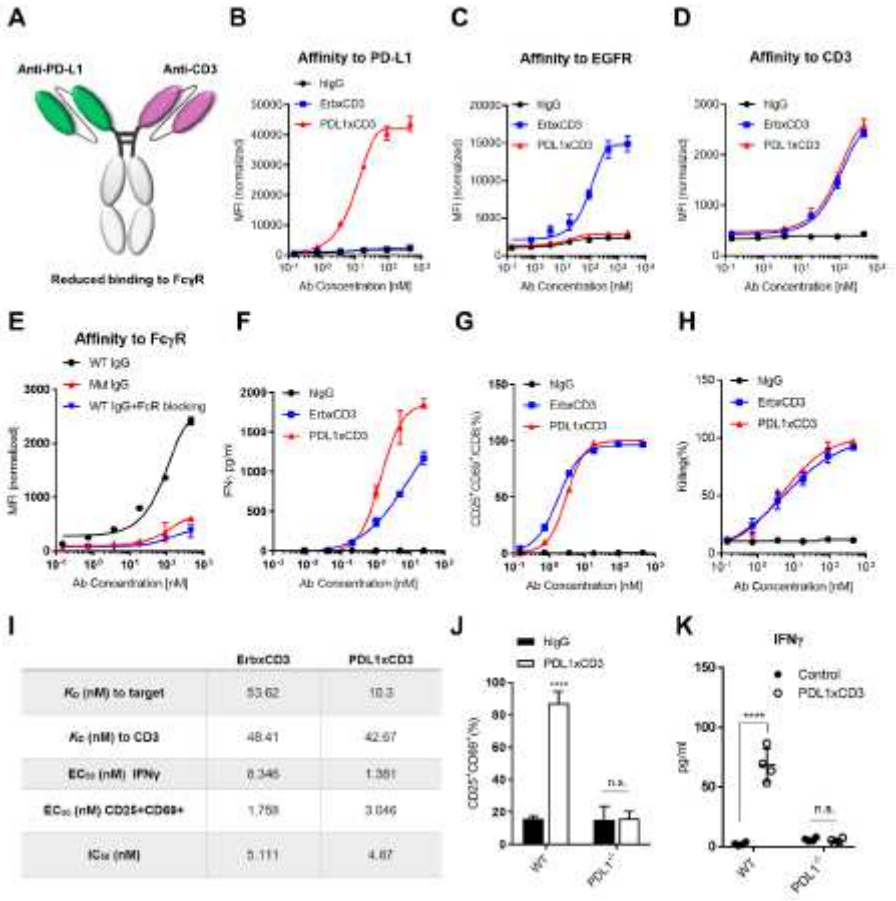

Figure 1

PDL1xCD3 targets PD-L1 to activate T cells in vitro. (A) Schematic structure of PDL1xCD3 bispecific antibody. PDL1xCD3 is composed of a single- chain variable fragment (ScFv) to PD-L1 and a ScFv to murine CD3ε, fused to a mutant human IgG1. (B) Binding of PDL1xCD3 to PD-L1 on MC38 cells overexpressing PD-L1. Cells were incubated with serial dilutions of PDL1xCD3, ErbxCD3, or human IgG control, followed by a fluorophore-conjugated anti-human IgG secondary antibody. Flow cytometry measured mean fluorescence intensity (MFI) (n=3). (C) Binding of PDL1xCD3 to EGFR on MC38 cells ectopically expressing chimeric EGFR (MC38E5). Cells were incubated with serial dilutions of PDL1xCD3, ErbxCD3, or human IgG control, followed by a fluorophore-conjugated anti-human IgG secondary antibody. Flow cytometry measured MFI (n=3). (D) Binding of PDL1xCD3 to CD3ε on CD8 T cells purified from mouse spleen. Cells were incubated with serial dilutions of PDL1xCD3, ErbxCD3, or human IgG control, followed by a fluorophore-conjugated anti-human IgG secondary antibody. Flow cytometry measured MFI (n=3). (E) Binding of PDL1xCD3 to FcγR on RAW 264.7 cells. Cells were incubated with serial dilutions of WT IgG fusion protein, mutant IgG fusion protein, or WT IgG fusion protein with anti-FcγR, followed by a fluorophore- conjugated anti-human IgG secondary antibody. Flow cytometry measured MFI (n=3). (F-H) MC38E5-GFP cells (3x104) and purified splenic CD8 T cells (3x105) were co-cultured with serial dilutions of PDL1xCD3, ErbxCD3, or human IgG control. IFNγ in the supernatant was

detected by cytokine beads array (CBA) (F). CD25 and CD69 expression on T cells were detected by flow cytometry (G). GFP+ 7AAD- tumor cells were detected by flow cytometry (H). (I) Summary of the KD, EC50 and IC50 of both antibodies. (J-K) Co-culture assay was performed with WT or PD-L1 KO MC38 as in (F), T cell activation (J) and IFNγ in the supernatant (K) were detected respectively. Data are shown as means ± SD, non-linear best fits for (B-H) and two-tailed unpaired t test for (J-729 K), ****P ≤ 0.0001. All experiments were repeated twice.

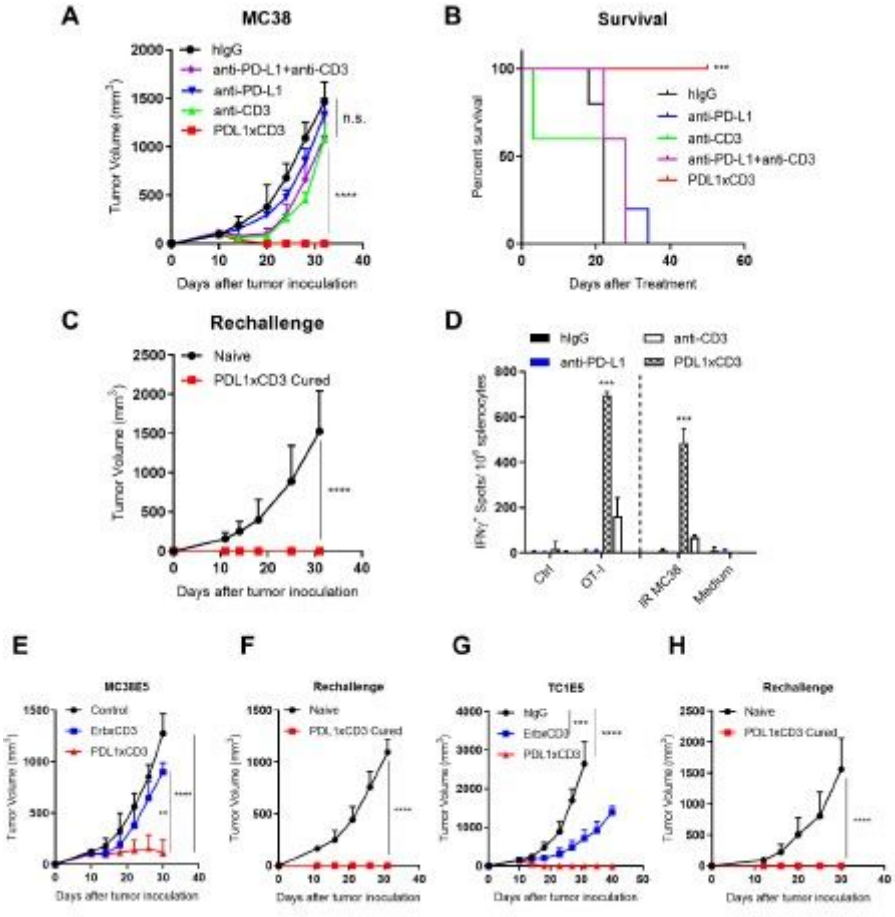

Figure 2

PDL1xCD3 generates superior anti-tumor effect than TAA-targeting BiTE in vivo. (A-C) C57BL/6J mice were subcutaneously inoculated with 1x106 MC38 tumor cells and treated with 0.25 mg/kg of fusion proteins twice on day 10 and 15. Tumor volume (A) and percentage of survival (B) was shown. (C) 50 days after PDL1xCD3 treatment, cured mice were re-challenged with 1x107 MC38 tumor cells. (D) C57BL/6J mice were subcutaneously inoculated with 1x106 MC38OVA tumor cells and treated as in panel A. 25 days after treatment, antigen specific T cells were detected by Elispot assay with splenocytes. (E-F) C57BL/6J mice were subcutaneously inoculated with 3x105 MC38E5 tumor cells and treated with 0.25 mg/kg of fusion proteins twice on day 10 and 15. (E) Tumor volume was measured twice per week. (F) 60 days post treatment, tumor free mice were re-challenged with 3x106 tumor cells. (G-H) C57BL/6J mice were subcutaneously inoculated with 1x106 TC1E5 tumor cells and treated with 0.25 mg/kg of fusion proteins twice on day 10 and 15. (G) Tumor volume was measured twice per week. (H) 60 days

post treatment, tumor free mice were re-challenged with 1x107 tumor cells. Data were shown as mean ± SEM (n=5) from two independent experiments. Statistical analysis was performed by two-way ANOVA and Log-rank test (B), **P ≤ 0.01, ***P ≤ 0.001, and ****P ≤ 0.0001.

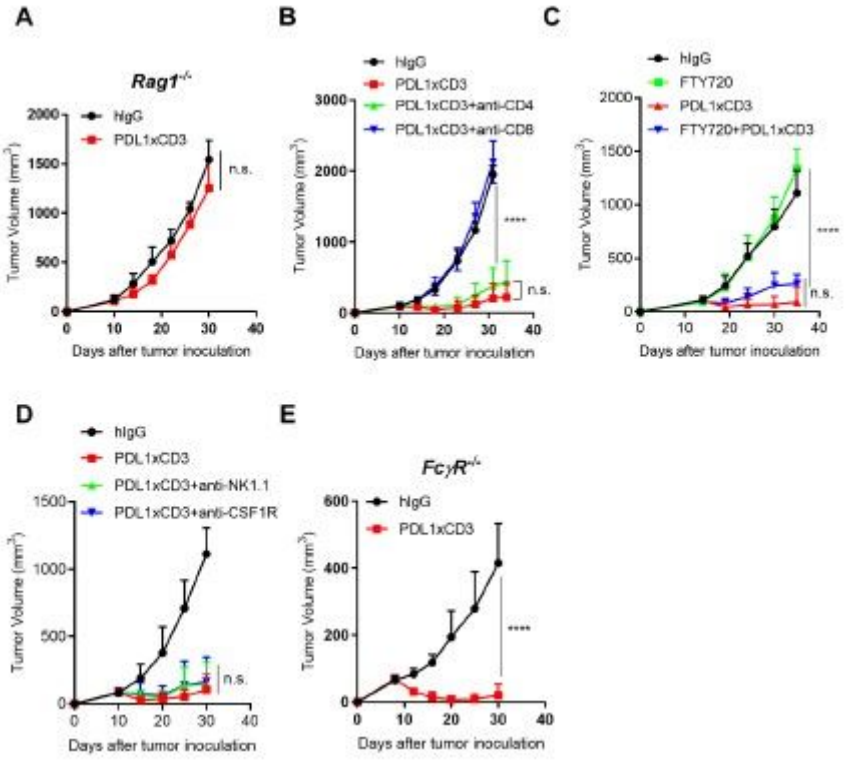

Figure 3

Pre-existing CD8 T cells are required for PDL1xCD3 treatment. (A) Rag1-/- mice were inoculated with 1x106 MC38 tumor cells and treated with PDL1xCD3 (0.25 mg/kg on day 10 and 15). (B) C57BL/6 mice were inoculated with 1x106 MC38 tumor cells and treated with PDL1xCD3 (0.25 mg/kg on day 10 and 15). 200µg anti-CD8 or anti-CD4 was administrated one day before treatment initiation and then twice a week for 2 weeks. (C) C57BL/6 mice were inoculated with 1x106 MC38 tumor cells and treated with PDL1xCD3 (0.25 mg/kg on day 14 and 18). 20µg FTY720 was administrated one day before treatment initiation and then 10µg every other day for 2 weeks. (D) C57BL/6 mice were inoculated with 1x106 MC38 tumor cells and treated with PDL1xCD3 (0.25 mg/kg on day 10 and 15). 200µg anti-NK1.1 or anti-CSF1R was administrated one day before treatment initiation and then twice a week for 2 weeks. (E) FcγR-/- mice were inoculated with 1x106 MC38 tumor cells and treated with PDL1xCD3 (0.25 mg/kg on day 8 and 12). Data were shown as mean ± SEM (n=5) from two independent experiments. Statistical analysis was performed by two-way ANOVA, ****P ≤ 0.0001.

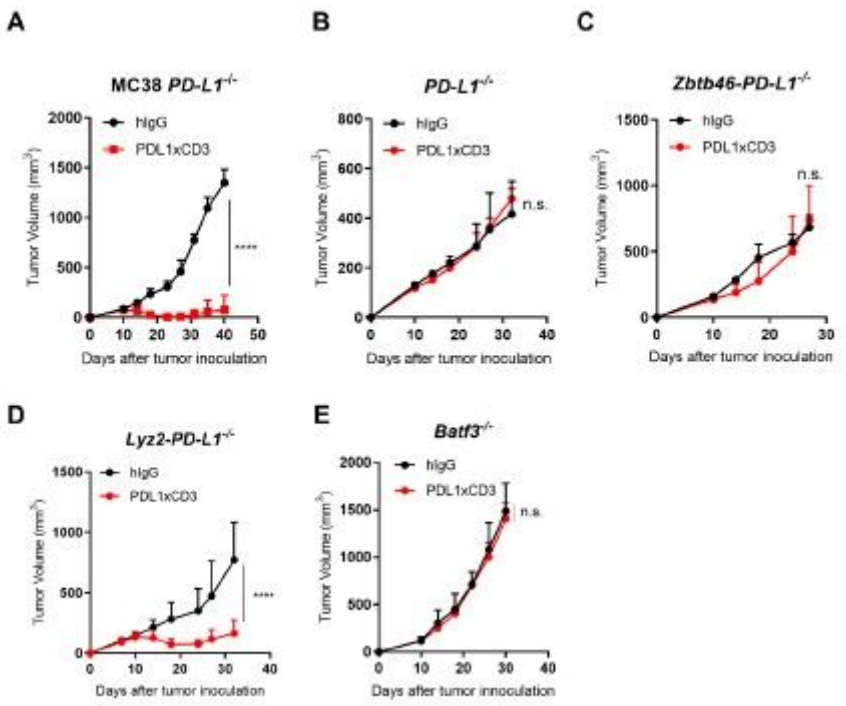

Figure 4

PD-L1 on dendritic cells is essential for the anti-tumor effect of PDL1xCD3. (A) C57BL/6J mice (n=5) were subcutaneously inoculated with 1x106 MC38-PDL1-/- tumor cells and treated with 0.25 mg/kg of fusion proteins twice on day 10 and 15. (B) PDL1-/- mice (n=5) were subcutaneously inoculated with 1x106 MC38 tumor cells and treated with 0.25 mg/kg of fusion proteins twice on day 10 and 15. (C) Zbtb46-Cre-PD-L1 f/f mice (n=5) were subcutaneously inoculated with 1x106 MC38 tumor cells and treated with 0.25 mg/kg of fusion proteins twice on day 10 and 15. (D) Lyz2-Cre-PD-L1 f/f mice (n=5) were subcutaneously inoculated with 1x106 MC38 tumor cells and treated with 0.25 mg/kg of fusion proteins twice on day 10 and 15. (E) Batf3-/- mice were inoculated with 1x106 MC38 tumor cells and treated with PDL1xCD3 (0.25 mg/kg on day 10 and 15). Data were shown as mean ± SEM from two independent experiments. Statistical analysis was performed by two-way ANOVA, ****P ≤ 0.0001.

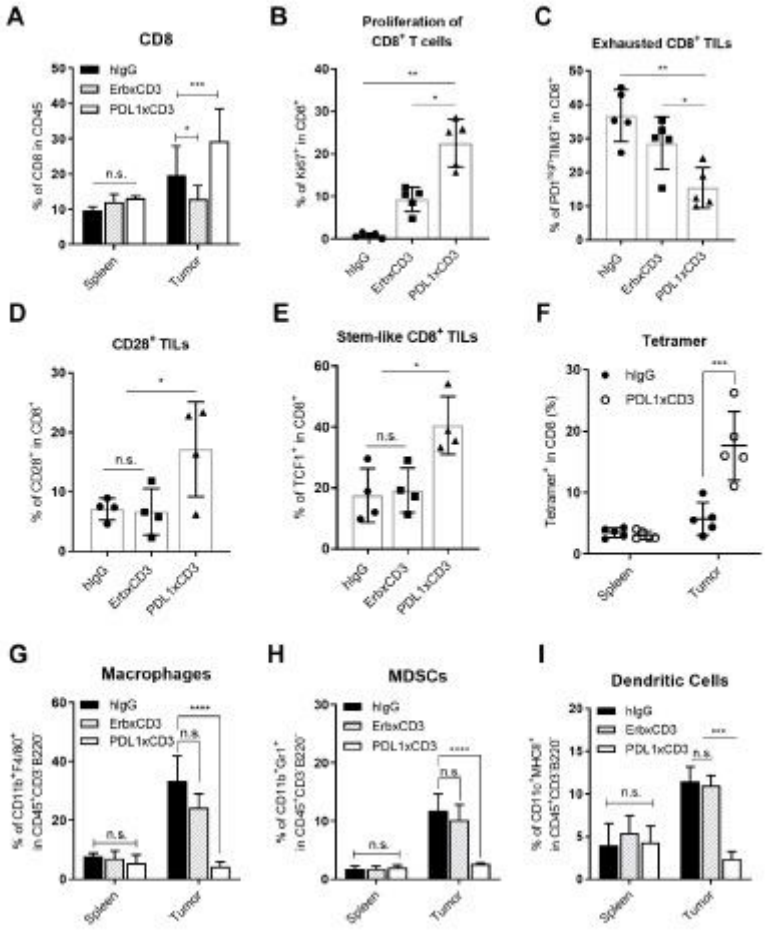

Figure 5

PDL1xCD3 reshapes a distinct immunophenotypic signature in tumor-bearing 774 mice. C57BL/6J mice (n=5) were subcutaneously inoculated with 1x106 MC38-OVA tumor cells and treated with 0.25 mg/kg of fusion proteins. Flow cytometry analysis was performed with splenocytes and dissociated tumor samples for the percentage of CD8 T cells (A), Ki-67+ CD8 T cells (B), PD-1high TIM-3+ CD8 T cells (C), CD28+ CD8 T cells (D), TCF1+ CD8 T cells (E), tetramer+ cells (F), F4/80+CD11b+ cells (G), Gr1+CD11b+ cells (H), MHC-II+CD11c+ cells (I). Representative result from two independent experiments were shown as mean ± SEM (n=5). Statistical analysis was performed by two-tailed unpaired t test, *P ≤ 0.05, **P ≤ 0.01, ***P ≤ 0.001, and ****P ≤ 0.0001.

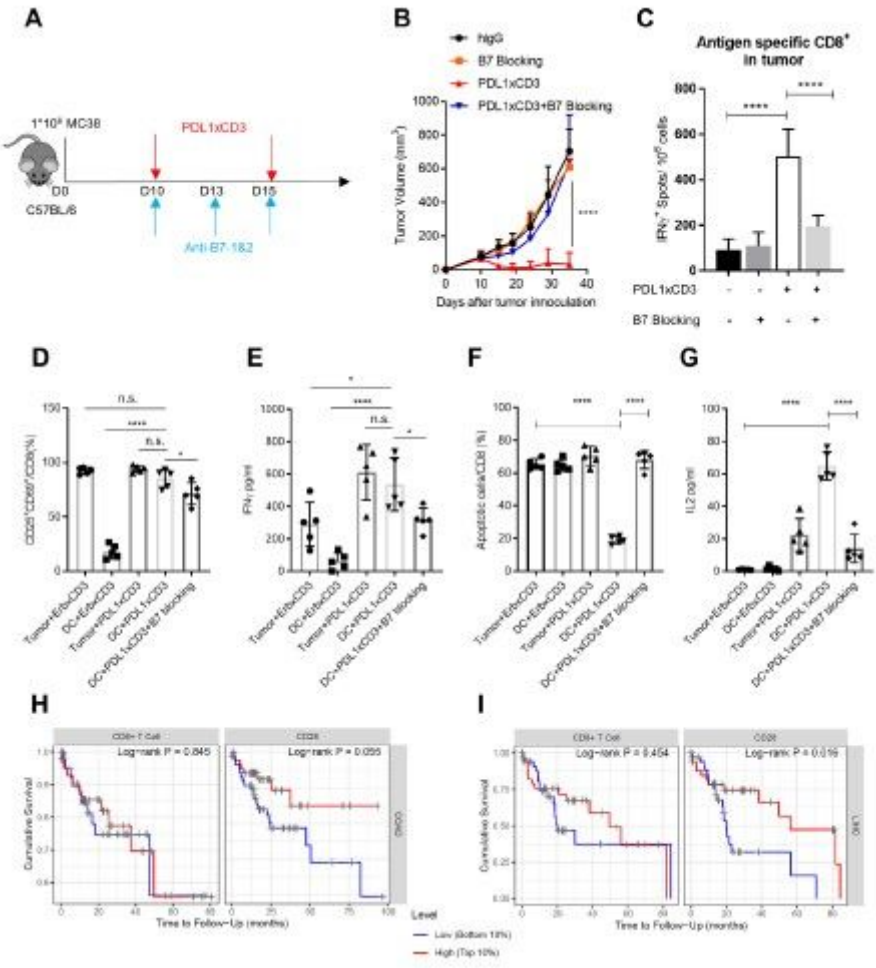

Figure 6

Co-stimulatory signaling is required for PDL1xCD3 mediated anti-tumor effects. (A-C) C57BL/6J mice were inoculated with 1x106MC38 tumor cells and treated with PDL1xCD3 (0.25 mg/kg on day 10 and 15), 200 μg anti-B7-1 and anti-B7-2 were administrated on day 10, 13, and 15. Experimental design (A). Tumor growth curve (B) and IFNγ-producing antigen specific CD8 T cells (C) were shown. (D-G) CD8 T cells were co-cultured with either tumor cells or dendritic cells in the presence of fusion proteins. T cell activation (D), supernatant IFNγ (E), apoptotic T cells (F) and supernatant IL2 (G) were measured by flow cytometry and CBA. (H-I) Cumulative survival in colorectal adenocarcinoma (COAD) and liver hepatocellular carcinoma(LIHC) patients according to CD8 infiltration and CD28 level in TCGA database. Representative result from two independent experiments were shown as mean ± SEM (n=5). Statistical analysis was performed by two-tailed unpaired t test (C-G), two-way ANOVA (B) and Log-rank test (H-I) *P ≤ 0.05, ****P ≤ 0.0001.